2011-06

String stability of multiple surface marine vessels

Angelopoulos, Christos K.

Monterey, California. Naval Postgraduate School

NAVAL POSTGRADUATE SCHOOL

MONTEREY, CALIFORNIA

THESIS

STRING STABILITY OF MULTIPLE SURFACE MARINE VESSELS

by

Christos K. Angelopoulos

June 2011

Thesis Advisor:	Fotis A. Papoulias
Second Reader:	Oleg A. Yakimenko

Approved for public release; distribution is unlimited

THIS PAGE INTENTIONALLY LEFT BLANK

REPORT DOCUMENTATION PAGE		Form Approved OMB No. 0704-0188

1. AGENCY USE ONLY *(Leave blank)*	2. REPORT DATE	3. REPORT TYPE AND DATES COVERED
	June 2011	Master's Thesis/Engineer's Thesis

4. TITLE AND SUBTITLE String Stability of Multiple Surface Marine Vessels	5. FUNDING NUMBERS
6. AUTHOR(S) Christos Angelopoulos	
7. PERFORMING ORGANIZATION NAME(S) AND ADDRESS(ES) Naval Postgraduate School Monterey, CA 93943-5000	8. PERFORMING ORGANIZATION REPORT NUMBER
9. SPONSORING /MONITORING AGENCY NAME(S) AND ADDRESS(ES) N/A	10. SPONSORING/MONITORING AGENCY REPORT NUMBER

11. SUPPLEMENTARY NOTES The views expressed in this thesis are those of the author and do not reflect the official policy or position of the Department of Defense or the U.S. Government. IRB Protocol number N/A.

12a. DISTRIBUTION / AVAILABILITY STATEMENT	12b. DISTRIBUTION CODE
Approved for public release; distribution is unlimited	A

13. ABSTRACT (maximum 200 words)

The phenomenon of string instability is well known in a platoon of cars moving forward in an Automated Highway System (AHS). It is also known that ships can experience a similar instability phenomenon from mis-coordination of guidance and control laws. The proposed research studies the latter phenomenon, generalized in the case of multiple marine surface vessels moving in a platoon. The question of how it is possible for ships traveling in formation to exhibit the phenomenon of string instability is answered. Moreover, we examine under what conditions this phenomenon can be exhibited, as well as how it can be prevented.

14. SUBJECT TERMS String stability, Platoon, Surface marine vessel, Path control, Control law, Guidance law, Eigenvalues, Damping ratio, Natural frequency	15. NUMBER OF PAGES 79
	16. PRICE CODE

17. SECURITY CLASSIFICATION OF REPORT	18. SECURITY CLASSIFICATION OF THIS PAGE	19. SECURITY CLASSIFICATION OF ABSTRACT	20. LIMITATION OF ABSTRACT
Unclassified	Unclassified	Unclassified	UU

NSN 7540-01-280-5500 Standard Form 298 (Rev. 2-89)
Prescribed by ANSI Std. 239-18

THIS PAGE INTENTIONALLY LEFT BLANK

Approved for public release; distribution is unlimited

STRING STABILITY OF MULTIPLE SURFACE MARINE VESSELS

Christos K. Angelopoulos
Lieutenant, Hellenic Navy
B.S., Hellenic Naval Academy, 2001

Submitted in partial fulfillment of the
requirements for the degree of

MASTER OF SCIENCE IN MECHANICAL ENGINEERING

and

MECHANICAL ENGINEER

from the

NAVAL POSTGRADUATE SCHOOL
June 2011

Author: Christos K. Angelopoulos

Approved by: Fotis A. Papoulias
Thesis Advisor

Oleg A. Yakimenko
Second Reader

Knox T. Millsaps
Chair, Department of Mechanical and Aerospace Engineering

THIS PAGE INTENTIONALLY LEFT BLANK

ABSTRACT

The phenomenon of string instability is well known in a platoon of cars moving forward in an Automated Highway System (AHS). It is also known that ships can experience a similar instability phenomenon from mis-coordination of guidance and control laws. The proposed research studies the latter phenomenon, generalized in the case of multiple marine surface vessels moving in a platoon. The question of how it is possible for ships raveling in formation to exhibit the phenomenon of string instability is answered. Moreover, we examine under what conditions this phenomenon can be exhibited, as well as how it can be prevented.

THIS PAGE INTENTIONALLY LEFT BLANK

TABLE OF CONTENTS

I. INTRODUCTION 1
A. MOTIVATION 1
B. BACKGROUND 3
C. OBJECTIVES 3
D. PATH CONTROL SYSTEM ARCHITECTURE 4
1. Kinds of Motion Stability 5
2. Need for Path Control 6
3. System Architecture 6

II. PROBLEM FORMULATION 9
A. INTRODUCTION 9
B. EQUATIONS OF MOTION 9
C. AUTOPILOT CONTROL LAW 13
1. Turning Dynamics 13
2. Control Law 15
D. EQUATIONS FOR GUIDANCE 17
E. COMBINED GUIDANCE AND CONTROL LAW 19
1. One Vessel 19
2. Two Vessels in a Platoon 21

III. STABILITY ANALYSIS 23
A. STABILITY OF ONE VESSEL 23
B. STRING STABILITY 24
1. Analytical Approach 24
2. Numerical Results 26
3. Effect of Damping Ratio ζ and Natural Frequency ω_n on Stability 29
4. Eigenvalues 40
5. Simulation 41

IV. CONCLUSIONS 45

APPENDIX A 47

APPENDIX B 49

LIST OF REFERENCES 63

INITIAL DISTRIBUTION LIST 65

THIS PAGE INTENTIONALLY LEFT BLANK

LIST OF FIGURES

Figure 1. Platoon of automated vehicles on an Automated Highway System, developed by the PATH project (From: [2]) 2
Figure 2. The kinds of motion stability (From: [9]) 5
Figure 3. Block-diagram representation of system architecture. Navigation compares actual and commanded path. Guidance provides the appropriate commanded heading angle ψ_C. ψ is the actual heading angle (From: [8]) 7
Figure 4. Either a fixed Cartesian coordinate system on the earth or a fixed system at the center of mass of the moving vessel can be used for deriving equations of motion 10
Figure 5. Behavior of actual rudder angle δ. This is not always the same with δ_0 that is delivered by the control law 16
Figure 6. The line of sight guidance scheme. The vessel has deviated from the commanded path x-axis and needs to direct its longitudinal axis toward a target point D to come back 18
Figure 7. Inertial deviation rate from the commanded path 18
Figure 8. Two vessels in a platoon, which have deviated from the commanded straight line path (x axis) . 21
Figure 9. Three stability diagrams for $\omega_{n_2} = 0.5\omega_{n_1}$ and $\zeta = 0.6, \zeta = 0.8, \zeta = 1.2$ respectively. Stability curves are drawn for $\omega_{n_1} = 1$ to 4.5 with step 0.5 . 31
Figure 10. Three stability diagrams for $\omega_{n_2} = \omega_{n_1}$ and $\zeta = 0.6, \zeta = 0.8, \zeta = 1.2$ respectively. Stability curves are drawn for $\omega_{n_1} = 1$ to 4.5 with step 0.5 . 33
Figure 11. Three stability diagrams for $\omega_{n_2} = 1.5\omega_{n_1}$ and $\zeta = 0.6, \zeta = 0.8, \zeta = 1.2$ respectively. Stability curves are drawn for $\omega_{n_1} = 1$ to 4.5 with step 0.5 . 35
Figure 12. A family of curves for the first vessel for different damping ratios from 0.4 to 1.2 and step 0.2. Natural frequency ω_{n_1} varies in the range 1-4.5 36
Figure 13. A family of curves for the second vessel for different damping ratios from 0.4 to 1.2 and step 0.2. Natural frequency ω_{n_1} varies in the

range 1-4.5 and ω_{n_2} in the range 0.5-2.25 ($\omega_{n_2} = 0.5\omega_{n_1}$) 37
Figure 14. A family of curves for the second vessel for different damping ratios from 0.4 to 1.2 and step 0.2. Natural frequency ω_{n_1} varies in the range 1-4.5 and ω_{n_2} in the range 1-4.5 ($\omega_{n_2} = \omega_{n_1}$) 38
Figure 15. A family of curves for the second vessel for different damping ratios from 0.4 to 1.2 and step 0.2. Natural frequency ω_{n_1} varies in the range 1-4.5 and ω_{n_2} in the range 1.5-6.75 ($\omega_{n_2} = 1.5\omega_{n_1}$) 39
Figure 16. Change of eigenvalues as $d_1 \to d_1^*$ 41
Figure 17. Change of deviation y_1, y_2 from the commanded path with time for stability conditions (I.C. $y_1 = 1, y_2 = 1.5$) 42
Figure 18. Change of deviation y_1, y_2 from the commanded path with time for stability conditions (I.C. $y_1 = -1, y_2 = 0$) 42
Figure 19. Change of deviation y_1, y_2 from the commanded path with time for stability conditions (I.C. $y_1 = 0, y_2 = 1$) 43
Figure 20. Change of deviation y_1, y_2 from the commanded path with time for stability conditions (I.C. $\psi_1 = 0.5, \psi_2 = 0.3$) 43
Figure 21. Change of deviation y_1, y_2 from the commanded path with time for stability conditions (I.C. $r_1 = 1$) 44

LIST OF TABLES

Table 1. Numerical results for: ξ 0.4 to 1.2, step 0.2. ω_{n_1} 1 to 4.5, step 0.1. d_1, d_2 0.05 to 2, step 0.01. $\frac{\omega_{n_1}}{\omega_{n_2}}$: 0.5, 1 or 1.5 49

THIS PAGE INTENTIONALLY LEFT BLANK

I. INTRODUCTION

A. MOTIVATION

The phenomenon of string instability is well known in a platoon of cars moving forward in an Automated Highway System (AHS), and it is also known that ships can experience a similar instability phenomenon. The main objective of an AHS is to increase the traffic flow capacity of highways. Other benefits are the increased safety, the time savings and the decrease in pollution. The increase of traffic flow capacity in particular is an imperative need due to the continuously expanding number of vehicles and the limited capacity of highways today.

A basic concept in an AHS is the formation of platoons or strings of vehicles. A platoon is a group of automated vehicles that maintain a tight spacing between themselves. In a platoon, each vehicle must safely follow its predecessor at a given distance [1]. The control system must guarantee the stability of all vehicles traveling together in the platoon. "The stability of groups of interconnected systems is known as string stability" [1].

Figure 1. Platoon of automated vehicles on an Automated Highway System, developed by the PATH project (From: [2])

Many researchers have studied the phenomenon of string instability observed in platoons in the case of an AHS. This phenomenon derives from delays in communication between systems, disturbances or generally mis-coordination phenomena. Marine surface vessels can experience a similar instability phenomenon from mis-coordination of guidance and control laws. The instability initiates when either a vessel deviates from the commanded path or cannot follow the speed changes of its predecessor.

Motivated by the case of cars, the proposed research studies the latter phenomenon, generalized in the case of multiple marine surface vessels moving in a platoon. The question of how it is possible for ships traveling in formation to exhibit the phenomenon of string instability is answered. Moreover, we examine under what conditions this phenomenon can be exhibited as well as how it can be prevented.

B. BACKGROUND

The phenomenon of string instability for multiple marine surface vessels has not been studied before. Nevertheless, it has been thoroughly studied in the case of AHS [3,1,4]. Moreover, there is previous work on path keeping of separated autonomous underwater vehicles [5,6,7]. Professor Papoulias has also analyzed the loss of stability for the case of one marine vehicle in the horizontal plane [8].

C. OBJECTIVES

Two vessels traveling in a platoon with constant speed in a straight line commanded path on the horizontal plane are considered. One or both vessels can deviate from the commanded path due to external disturbances such as a big wave, and this could lead to string instability phenomena from mis-coordination of guidance and control laws.

The purpose of this study is to examine these instabilities. Specifically, the objectives of the study are:

a) To explain a path control system's architecture

b) To introduce a mathematical model based on a proposed autopilot control law in coordination with a guidance law

c) To carry out a stability analysis for the vessels traveling in a platoon

d) To examine under what conditions the phenomenon of string instability can be exhibited and how it can be prevented

This thesis contains four chapters. In Chapter I, the need for an accurate path control system as well as the architecture of such a system is explained. Chapter II develops a mathematical formulation of the problem. The equations of motion in a horizontal plane are derived. Nomoto's model is used to provide the basis for an autopilot control law that stabilizes the vessel to a commanded heading angle ψ_C, capable of restoring the vessel to the commanded path. The line of sight guidance scheme is used in coordination with the control law, and the combined guidance and control law is derived. Chapter III presents a stability analysis for two different cases: of one vessel and the string based on the particular natural frequencies ω_n, the damping ratios ζ of each autopilot and the guidance preview distances d_1, d_2. Criteria for stability and conclusions about the effect of damping ratio ζ and natural frequency ω_n are drawn. A simulation verifies the results.

D. PATH CONTROL SYSTEM ARCHITECTURE

Ship dynamics is a field that involves both maneuverability (controllability) and motion in waves (seakeeping). Maneuverability is the capability of the ship to change direction as a result of actions taken by the helmsman or the autopilot. Maneuvering characteristics of ships are complex phenomena, which include course keeping and turning ability. These are conflicting objectives. A vessel that is very stable and keeps well its course will display a hardness of turning. On the other hand, a vessel with enhanced turning ability will be unstable on course and will turn unintentionally due to environmental disturbances [9].

1. Kinds of Motion Stability

Path course keeping and motion stability are closely related. Generally, we can classify the different kinds of motion stability of a marine surface vessel by examining the response on an external disturbance. In Figure 2, the vessel is initially considered to have a straight-line motion with a constant speed (nominal condition) before a disturbance is applied. As it is implied, the simplest kind of motion stability is the straight-line (dynamic) stability in which the vessel continues to move in a straight line after release from a disturbance but at a different direction. In another case, the directional stability, the vessel maintains not only its straight-line motion but its direction too. Finally, in positional motion stability, the vessel acquires its original path (with the same direction) [9].

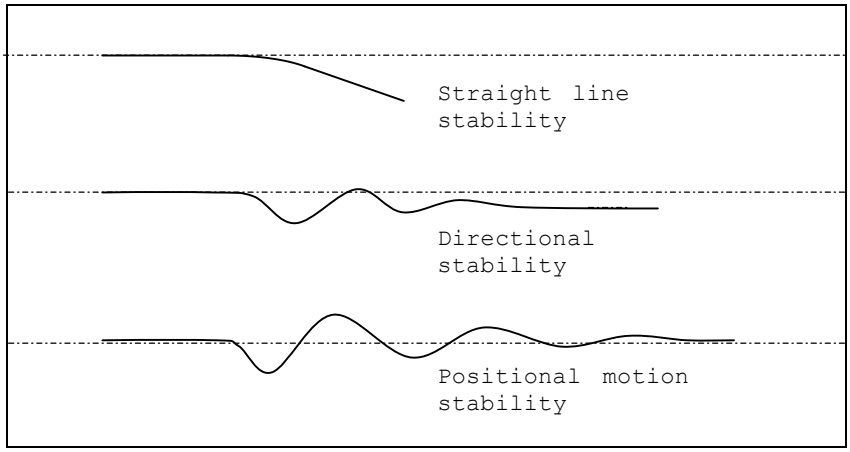

Figure 2. The kinds of motion stability (From: [9])

2. Need for Path Control

The need for accurate path control arises in naval applications. Common practice for ships is to move on prescribed routes. The helmsman normally is called to deliver the ship's appropriate heading angle and yaw velocity. Path accuracy is particularly important when the ship has to operate in confined waters. Furthermore,

> small unmanned marine vehicles suitable for use in both naval and commercial operations have unique mission requirements and dynamic response characteristics. In particular, they are required to be highly maneuverable and very responsive as they operate in obstacle-avoidance and object-recognition scenarios. [10]

Therefore, accurate path control in confined or shoal waters, as well as in open sea, is an imperative need, which path control systems are called upon to satisfy.

3. System Architecture

A system with path control capabilities, in general, can be assumed to consist of three main dynamic systems that are navigation, guidance and autopilot loops, as depicted schematically in Figure 3. The navigation loop processes actual geographical position and heading information (ψ) to provide the actual path. The latter is compared with the commanded path, which comes from path planning operations, to create the positional error. The guidance loop is fed with positional error and generates an appropriate commanded heading angle (ψ_C) capable of

restoring the vessel to the commanded path. The autopilot feedback loop is called upon to deliver this commanded angle [8].

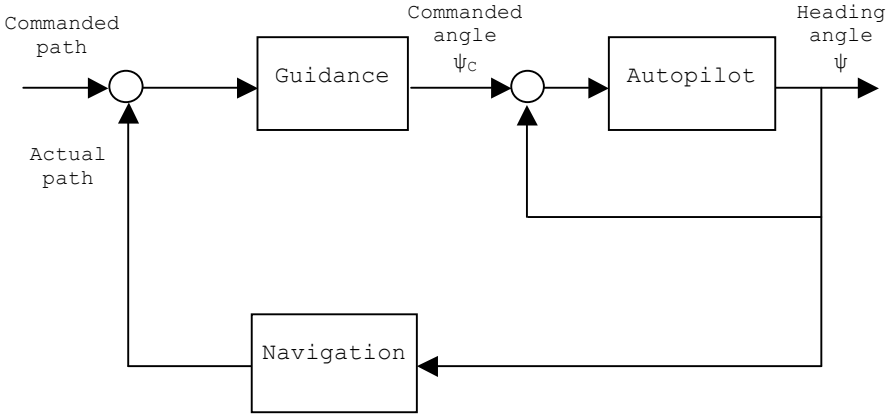

Figure 3. Block-diagram representation of system architecture. Navigation compares actual and commanded path. Guidance provides the appropriate commanded heading angle ψ_C. ψ is the actual heading angle (From: [8])

THIS PAGE INTENTIONALLY LEFT BLANK

II. PROBLEM FORMULATION

A. INTRODUCTION

This chapter introduces a mathematical model for the problem of path keeping. Equations of motion for a marine surface vessel during maneuvering in a horizontal plane will result in the basic turning dynamics of the vessel. Based on these dynamics, we suggest a control law for the autopilot, which in coordination with an appropriate guidance scheme stabilizes the vessel to a commanded heading angle ψ_C capable of restoring the vessel to the commanded path. Finally, we arrive at the systems of equations that describe the behavior of two vessels moving in a platoon in vector form, or at the combined guidance and control law.

B. EQUATIONS OF MOTION

Maneuvering characteristics of a marine surface vessel can be described by the equations of motion. These equations can be derived by Newton's second law and are the basis for the autopilot control law.

The vessel is considered to be a rigid body with only three degrees of freedom—surge, sway and yaw—and which moves in the horizontal plane. The other three degrees of freedom—roll, pitch and heave—are neglected and not considered in this treatment. The equations can be considered either with reference to a fixed Cartesian coordinate system on the earth or a fixed system at the center of mass of the moving vessel, as illustrated in

Figure 4. Yaw angle ψ, is the angle between the ship's longitudinal axis x and the fixed axis x_0. Furthermore, r is the yaw velocity ($r = \dot{\psi}$). Newton's law expressed in a fixed Cartesian coordinate system gives

$$\begin{aligned} m\ddot{x}_0 &= X_0 \\ m\ddot{y}_0 &= Y_0 \\ I_z\ddot{\psi} &= N \quad \text{or} \quad I_z\dot{r} = N \end{aligned} \tag{1}$$

where X_0: the total force in x_0 direction

Y_0: the total force in y_0 direction

N: the moment about z_0 axis

m: the vessel's mass

I_z: the moment of inertia about z_0 axis

$\ddot{x}_0, \ddot{y}_0$: acceleration in x_0, y_0 directions

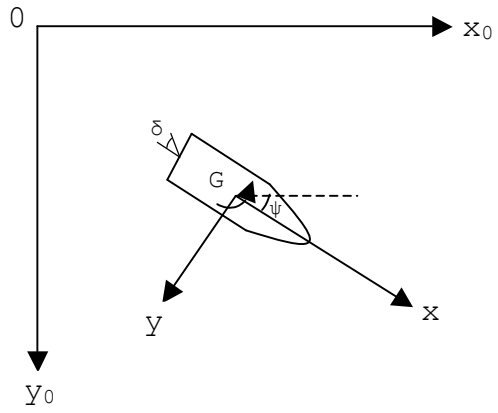

Figure 4. Either a fixed Cartesian coordinate system on the earth or a fixed system at the center of mass of the moving vessel can be used for deriving equations of motion

Equations (1) are written with respect to a fixed coordinate system at a particular place. To dispose of this limitation, it is more convenient to express them with respect to a fixed system on the moving vessel. This will be a counterclockwise system, with the *x* positive axis in the longitudinal direction and the *y* positive axis at the starboard of the vessel (Figure 4). The previous equations become [9]

$$\begin{aligned} m\dot{u} - mvr &= X \\ m\dot{v} + mur &= Y \\ I_z \dot{r} &= N \end{aligned} \tag{2}$$

where u: the surge velocity

v: the sway velocity

r: the yaw velocity

X: the total force in *x* direction

Y: the total force in *y* direction

Equations (2) can subsequently be written with respect to a fixed system at amidships instead of the center of mass of the vessel [9]

$$\begin{aligned} m(\dot{u} - vr - x_G r^2) &= X \\ m(\dot{v} + ur + x_G \dot{r}) &= Y \\ I_Z \dot{r} + m x_G (\dot{v} + ur) &= N \end{aligned} \tag{3}$$

where x_G: the x-coordinate of the center of mass G.

Total forces and moments in Equations (3), which act during maneuvering, are composed of fluid forces components due to surrounding water, forces due to control surfaces (rudders, bow planes, thrusters), forces due to environment (wind, current, waves) and the propulsion force (T)

$$X = X_F + X_S + X_E + T$$

$$Y = Y_F + Y_S + Y_E \tag{4}$$

$$N = N_F + N_S + N_E$$

where X_F, Y_F, N_F: the fluid forces components

X_S, Y_S, N_S: the control surfaces forces components

X_E, Y_E, N_E: the environment forces components

At this point, if we consider a nominal condition for the vessel that is the straight line motion at constant speed U, according to [9], the fluid forces components can be expressed in the following form

$$\begin{aligned} X_F &= \frac{\partial X_F}{\partial \dot{u}}\dot{u} + \frac{\partial X_F}{\partial u}(u-U) \\ Y_F &= \frac{\partial Y_F}{\partial v}v + \frac{\partial Y_F}{\partial \dot{v}}\dot{v} + \frac{\partial Y_F}{\partial r}r + \frac{\partial Y_F}{\partial \dot{r}}\dot{r} \\ N_F &= \frac{\partial N_F}{\partial v}v + \frac{\partial N_F}{\partial \dot{v}}\dot{v} + \frac{\partial N_F}{\partial r}r + \frac{\partial N_F}{\partial \dot{r}}\dot{r} \end{aligned} \tag{5}$$

and the control surfaces forces components are expressed

$$\begin{aligned} X_S(\delta) &= X_S(0) + \frac{\partial X_S}{\partial \delta}\delta = 0 \\ Y_S(\delta) &= Y_S(0) + \frac{\partial Y_S}{\partial \delta}\delta = Y_\delta \delta \\ N_S(\delta) &= N_S(0) + \frac{\partial N_S}{\partial \delta}\delta = N_\delta \delta \end{aligned} \tag{6}$$

where δ : the rudder angle

U: the nominal velocity in x direction

Assuming no environmental forces and substituting Equations (4),(5),(6) into Equation (3), we arrive at the following sway and yaw linear equations of motion in the horizontal plane

$$\begin{aligned}(m-Y_{\dot{v}})\dot{v}-(Y_{\dot{r}}-mx_G)\dot{r} &= Y_v v+(Y_r-mu)r+Y_\delta\delta \\ (I_Z-N_{\dot{r}})\dot{r}-(N_{\dot{v}}-mx_G)\dot{v} &= N_v v+(N_r-mx_G u)r+N_\delta\delta\end{aligned} \tag{7}$$

By nondimensionalizing the above equation in terms of water density ρ, vessel length L, and nominal velocity U, we take the dimensionless form that has the same identical form [9]

$$\begin{aligned}(m-Y_{\dot{v}})\dot{v}-(Y_{\dot{r}}-mx_G)\dot{r} &= Y_v v+(Y_r-m)r+Y_\delta\delta \\ (I_Z-N_{\dot{r}})\dot{r}-(N_{\dot{v}}-mx_G)\dot{v} &= N_v v+(N_r-mx_G)r+N_\delta\delta\end{aligned} \tag{8}$$

C. AUTOPILOT CONTROL LAW

Sway and yaw dimensionless equations of motion (8) yield the basic turning dynamics of a marine surface vessel. Moreover, a control law, based on these dynamics, is needed for the autopilot so that vessel's stabilization to any commanded heading angle ψ_c becomes achievable.

1. Turning Dynamics

Re-working the sway-yaw Equations (8), the following second-order linear differential equations are obtained [9]

$$\begin{aligned}T_1T_2\ddot{r}+(T_1+T_2)\dot{r}+r &= K\delta+KT_3\dot{\delta} \\ T_1T_2\ddot{v}+(T_1+T_2)\dot{v}+v &= K_v\delta+K_vT_4\dot{\delta}\end{aligned} \tag{9}$$

where $T_1T_2 = \dfrac{(Y_{\dot v}-m)(N_{\dot r}-I_z)-(Y_{\dot r}-mx_G)(N_{\dot v}-mx_G)}{Y_v(N_r-mx_GU)-N_v(Y_r-mU)}$

$$T_1+T_2 = \frac{(Y_{\dot v}-m)(N_r-mx_GU)+Y_v(N_{\dot r}-I_z)}{Y_v(N_r-mx_GU)-N_v(Y_r-mU)} - \frac{(Y_{\dot r}-mx_G)N_v+(Y_r-mU)(N_{\dot v}-mx_G)}{Y_v(N_r-mx_GU)-N_v(Y_r-mU)}$$

$$T_3 = \frac{Y_\delta(N_{\dot v}-mx_G)-N_\delta(Y_{\dot v}-m)}{Y_\delta N_v - N_\delta Y_v}$$

$$T_4 = \frac{Y_\delta(N_{\dot r}-I_z)-N_\delta(Y_{\dot r}-mx_G)}{Y_\delta(N_r-mx_GU)-N_\delta(Y_r-mU)}$$

$$K = \frac{Y_\delta N_v - N_\delta Y_v}{Y_v(N_r-mx_GU)-N_v(Y_r-mU)}$$

$$-K_v = \frac{Y_\delta(N_r-mx_GU)-N_\delta(Y_r-mU)}{Y_v(N_r-mx_GU)-N_v(Y_r-mU)}$$

The first of the above ordinary linear differential equations describes apparently the relationship between rudder angle δ and yaw velocity r. The transfer function between r, δ can be obtained from this equation simply by writing the Laplace transformation

$$L(T_1T_2\ddot r)+L((T_1+T_2)\dot r)+L(r)=L(K\delta)+L(KT_3\dot\delta)$$

or

$$\frac{r}{\delta}=\frac{K+KT_3s}{T_1T_2s^2+(T_1+T_2)s+1} \qquad (10)$$

where r, δ: the Laplace transformations of time-dependent variables.

Performing a Taylor series expansion in s and keeping the first order terms, Equation (10) reduces to a decipherable first order transfer function [8]

$$\frac{r}{\delta}=\frac{b}{s-a} \qquad (11)$$

where $b = \frac{K}{T} = \frac{K}{T_1 + T_2 - T_3}$

$$a = -\frac{1}{T} = -\frac{1}{T_1 + T_2 - T}$$

$$T = T_1 + T_2 - T_3$$

or in differential form

$$\dot{r} = ar + b\delta \tag{12}$$

The last equation is called Nomoto's first order model and embodies the radical characteristic of turning in a particularly useful form since no sway velocity feedback is necessary.

So far, we have concluded that the vessel turning dynamics can be described by Equation (12) and

$$\dot{\psi} = r \tag{13}$$

2. Control Law

Autopilot is intended to deliver the appropriate commanded heading angle ψ_C, capable of restoring the vessel to the commanded path. But the rudder angle δ in Nomoto's equation is the actual rudder angle, which is not always the same as the one that is delivered by the autopilot. Actually, the rudder angle δ has a value δ_0 that is given by a linear rudder angle control law, which will be discussed later, until δ_0 reaches a particular limit. Above this limit, δ is considered to be equal to a saturation value δ_{sat} (Figure 5). This saturation value is typically set at *0.4 radians*.

$\delta=\delta_0$, *if* $|\delta_0| \leq 0,4$ *rad*

or (14)

$\delta=\delta_{sat}$, *if* $|\delta_0| > 0,4$ *rad*

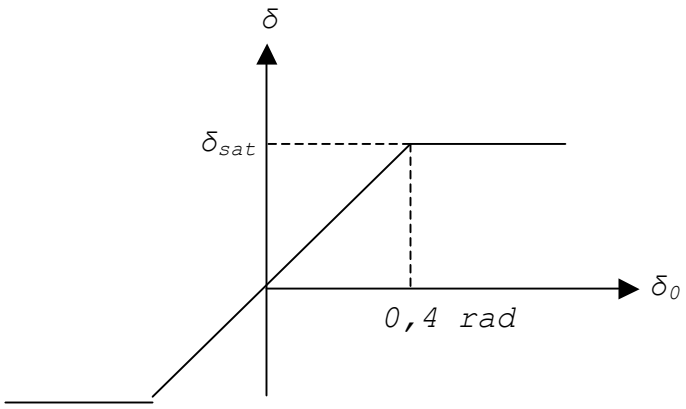

Figure 5. Behavior of actual rudder angle δ. This is not always the same with δ_0 that is delivered by the control law

The above behavior of rudder angle δ can be demonstrated simply by the hyperbolic tangent function

$$\delta = \delta_{sat} \tanh(\frac{\delta_0}{\delta_{sat}}) \tag{15}$$

The linear feedback heading control law, which will be incorporated into the autopilot, is based on Equation (12), and is of the form [8]

$$\delta_0 = k_1(\psi - \psi_c) + k_2 r \tag{16}$$

The system's transfer function is obtained from Equations (12), (13), and (16) as

$$\frac{\psi}{\psi_c} = \frac{-bk_1}{s^2 - (a + bk_2)s - bk_1} \tag{17}$$

This transfer function stabilizes the vessel to any commanded heading angle ψ_c. The system characteristic equation is

$$s^2 - (a + bk_2)s - bk_1 = 0 \tag{18}$$

Comparing the characteristic equation with the standard form for the second-order system

$$s^2 + 2\zeta\omega_n s + \omega_n{}^2 = 0 \tag{19}$$

the controller gains can be computed as

$$\begin{aligned} k_1 &= -\frac{\omega_n{}^2}{b} \\ k_2 &= -\frac{a + 2\zeta\omega_n}{b} \end{aligned} \tag{20}$$

The gains can be determined from the desired values of ω_n, ζ. These are selected based on general guidelines for second-order system transient response.

D. EQUATIONS FOR GUIDANCE

The autopilot, using the previous control law, stabilizes the vessel to an appropriate commanded heading angle ψ_c. This angle is generated by a dynamical system called guidance. In this section, we determine this angle.

The line of sight guidance scheme [8] is illustrated in Figure 6. According to this, the vessel is located at *(x,y)* at a distance *y* from the commanded straight-line path that is the *x*-axis. Trying to come back to the commanded path, the vessel attempts to direct its longitudinal axis toward a target point *D* that is located ahead of the vessel

at a distance *d* on the vessel's nominal path. In this case, the commanding heading angle ψ_c is the line of sight angle

$$\psi_C = -\tan^{-1}\frac{y}{d} \tag{21}$$

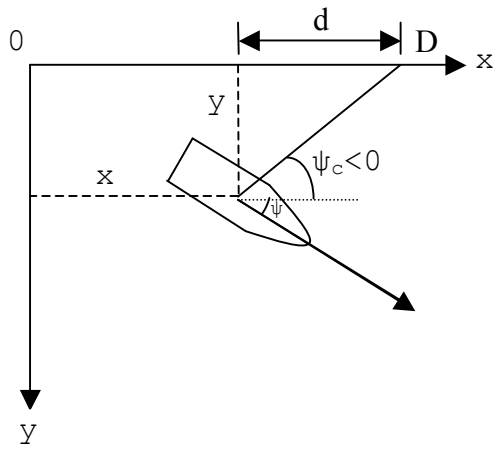

Figure 6. The line of sight guidance scheme. The vessel has deviated from the commanded path *x*-axis and needs to direct its longitudinal axis toward a target point *D* to come back

Furthermore, this guidance law is based on the inertial deviation rate from the commanded path (Figure 7)

$$\dot{y} = \sin\psi \tag{22}$$

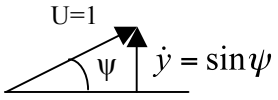

Figure 7. Inertial deviation rate from the commanded path

According to this guidance law, the commanded heading angle is not constant but a function of the vessel's position and the distance *d*. A change in distance *d* can

affect the speed of guidance law response. However, the autopilot has a limited reaction time according to the specified natural frequency ω_n and damping ratio ζ. Thus, parameter d must be chosen properly in order for the desired response to be achieved.

E. COMBINED GUIDANCE AND CONTROL LAW

In this section, we derive the combined guidance and control law that describes the behavior of a vessel that has deviated from the commanded straight-line path and tries to return by following a target point D (Figure 6). Afterwards, we expand for two vessels moving in a platoon.

1. One Vessel

The control law (Equation (16)) including the guidance scheme (Equation (21)) becomes

$$\delta_0 = k_1(\psi + \tan^{-1}\frac{y}{d}) + k_2 r \tag{23}$$

The linearized form of this equation, for very small heading angle ψ_C , is

$$\delta_0 = k_1(\psi + \frac{y}{d}) + k_2 r \tag{24}$$

Nomoto's Equation (12) combined with Equations (15) and (24) gives

$$\dot{r} = ar + b\delta_{sat}\tanh(\frac{1}{\delta_{sat}}k_1(\psi + \frac{y}{d}) + k_2 r) \tag{25}$$

Then, the system of equations that describes the behavior of the complete system, including the autopilot control law along with the guidance scheme, is given by [8]

$$\begin{aligned}\dot{\psi} &= r \\ \dot{r} &= ar + b\delta_{sat}\tanh(\frac{1}{\delta_{sat}}k_1(\psi + \frac{y}{d}) + k_2 r) \\ \dot{y} &= \sin\psi\end{aligned} \tag{26}$$

or in linearized form

$$\begin{aligned}\dot{\psi} &= r \\ \dot{r} &= ar + b(k_1(\psi + \frac{y}{d}) + k_2 r) \\ \dot{y} &= \psi\end{aligned} \tag{27}$$

It is desirable to write the above system as a matrix Equation [8]

$$\dot{x} = Ax \tag{28}$$

where $x = [\psi, r, y]^T$ and $A = \begin{bmatrix} 0 & 1 & 0 \\ bk_1 & a + bk_2 & \frac{bk_1}{d} \\ 1 & 0 & 0 \end{bmatrix}$

Finally, from Equations (20), it is

$$\begin{aligned} bk_1 &= -\omega_n^2 \\ a + bk_2 &= -2\zeta\omega_n \end{aligned} \tag{29}$$

and matrix A reforms to

$$A = \begin{bmatrix} 0 & 1 & 0 \\ -\omega_n^2 & -2\zeta\omega_n & -\frac{\omega_n^2}{d} \\ 1 & 0 & 0 \end{bmatrix} \tag{30}$$

2. Two Vessels in a Platoon

Now we expand the previous concept for two vessels. In this case, the first vessel attempts to direct its longitudinal axis toward a target point D, whereas the second vessel points its longitudinal axis toward the first one (Figure 8). In this consideration, d_1 is the distance between the target point *D* and the first vessel, and d_2 the distance between the two vessels always measured on the commanded path.

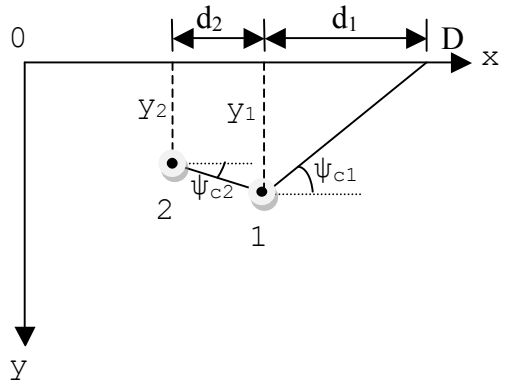

Figure 8. Two vessels in a platoon, which have deviated from the commanded straight line path (x axis)

The systems of equations that describe both vessels are

$$\begin{aligned} \dot{\psi}_1 &= r_1 & & & \dot{\psi}_2 &= r_2 \\ \dot{r}_1 &= a_1 r_1 + b_1\left(k_{11}\left(\psi_1 + \frac{y_1}{d_1}\right) + k_{21} r_1\right) & \text{and} & & \dot{r}_2 &= a_2 r_2 + b_2\left(k_{12}\left(\psi_2 + \frac{y_2}{d_2}\right) + k_{22} r_2\right) \\ \dot{y}_1 &= \psi_1 & & & \dot{y}_2 &= \psi_2 \end{aligned} \qquad (31)$$

or

$$\dot{x} = Ax \qquad (32)$$

where $x = [\psi_1, r_1, y_1, \psi_2, r_2, y_2]^T$, $A = \begin{bmatrix} 0 & 1 & 0 & 0 & 0 & 0 \\ b_1 k_{11} & a_1 + b_1 k_{21} \frac{b_1 k_{11}}{d_1} & 0 & 0 & 0 & \\ 1 & 0 & 0 & 0 & 0 & 0 \\ 0 & 0 & 0 & 0 & 1 & 0 \\ 0 & 0 & \frac{-b_2 k_{12}}{d_2} & b_2 k_{12} & a_2 + b_2 k_{22} & \frac{b_2 k_{12}}{d_2} \\ 0 & 0 & 0 & 1 & 0 & 0 \end{bmatrix}$

III. STABILITY ANALYSIS

In this chapter, we analyze the problem of stability for two vessels moving in a string with constant speed on a straight-line commanded path (trivial equilibrium solution characterized by $\psi=r=y=0$). One or both vessels can deviate from the commanded path due to external disturbances such as a big wave. This is translated to some initial conditions others than the trivial solution. The system can lead to string instability phenomena from mis-coordination of guidance and control laws. Specific criteria for string stability, and conclusions about the effect of damping ratio ζ and natural frequency ω_n are drawn. A simulation verifies the results. But before we study the string, we look at the previous case of one vessel trying to remain on the commanded path (Figure 6).

A. STABILITY OF ONE VESSEL

For the case of one vessel, we have already referred to the combined guidance and control law, Equation (28), and the matrix A

$$A = \begin{bmatrix} 0 & 1 & 0 \\ -\omega_n^2 & -2\zeta\omega_n & -\dfrac{\omega_n^2}{d} \\ 1 & 0 & 0 \end{bmatrix} \tag{30}$$

Local stability properties can then be established by the eigenvalues of matrix A [8]. The characteristic equation of A is

$$\lambda^3 + 2\zeta\omega_n\lambda^2 + \omega_n{}^2\lambda + \frac{\omega_n{}^2}{d} = 0 \tag{33}$$

If we neglect the constant term $\frac{\omega_n{}^2}{d}$ from Equation (33), i.e., $d \to \infty$ or the guidance law is eliminated, Equation (33) reduces to Equation (19) (i.e., the characteristic equation when control law stabilizes the vessel to any commanded heading angle ψ_c without the presence of the guidance law).

Applying Routh's criterion to Equation (33) we have

$$2\zeta\omega_n{}^3 - \frac{\omega_n{}^2}{d} > 0 \Rightarrow d > \frac{1}{2\zeta\omega_n}$$

or

$$d_{critical} = \frac{1}{2\zeta\omega_n} \tag{34}$$

For $d > \frac{1}{2\zeta\omega_n}$ eigenvalues of A have negative real parts and the combined guidance and control law provides stability, i.e., the vessel follows the commanded path.

B. STRING STABILITY

1. Analytical Approach

The controller gains for the first vessel are (from Equations (20))

$$\begin{aligned} k_{11} &= \frac{-\omega_{n_1}{}^2}{b_1} \\ k_{21} &= \frac{-(a_1 + 2\zeta_1\omega_{n_1})}{b_1} \end{aligned} \tag{35}$$

and for the second vessel

$$k_{12} = \frac{-\omega_{n_2}{}^2}{b_2}$$
$$k_{22} = \frac{-(a_2 + 2\zeta_2\omega_{n_2})}{b_2} \qquad (36)$$

Using the previous values for gains, matrix A in Equation (32) turns to be

$$A = \begin{bmatrix} 0 & 1 & 0 & 0 & 0 & 0 \\ -\omega_{n_1}{}^2 & -2\zeta_1\omega_{n_1} & \frac{-\omega_{n_1}{}^2}{d_1} & 0 & 0 & 0 \\ 1 & 0 & 0 & 0 & 0 & 0 \\ 0 & 0 & 0 & 0 & 1 & 0 \\ 0 & 0 & \frac{\omega_{n_2}{}^2}{d_2} & -\omega_{n_2}{}^2 & -2\zeta_2\omega_{n_2} & \frac{-\omega_{n_2}{}^2}{d_2} \\ 0 & 0 & 0 & 1 & 0 & 0 \end{bmatrix} \qquad (37)$$

The study of the eigenvalues of matrix A can reveal the local stability properties of the string. Especially, the characteristic equation of matrix A

$$\begin{aligned} &\lambda^6 + 2(\zeta_1\omega_{n_1} + \zeta_2\omega_{n_2})\lambda^5 + (\omega_{n_1}{}^2 + \omega_{n_2}{}^2 + 4\zeta_1\zeta_2\omega_{n_1}\omega_{n_2})\lambda^4 + \\ &\left(\frac{\omega_{n_1}{}^2}{d_1} + \frac{\omega_{n_2}{}^2}{d_2} + 2\zeta_1\omega_{n_1}\omega_{n_2}{}^2 + 2\zeta_2\omega_{n_1}{}^2\omega_{n_2}\right)\lambda^3 + \\ &\left(2\zeta_1\omega_{n_1}\frac{\omega_{n_2}{}^2}{d_2} + 2\zeta_2\frac{\omega_{n_1}{}^2}{d_1}\omega_{n_2} + \omega_{n_1}{}^2\omega_{n_2}{}^2\right)\lambda^2 + \\ &\left(\omega_{n_1}{}^2\frac{\omega_{n_2}{}^2}{d_2} + \frac{\omega_{n_1}{}^2}{d_1}\omega_{n_2}{}^2\right)\lambda + \frac{\omega_{n_1}{}^2\omega_{n_2}{}^2}{d_1 d_2} = 0 \end{aligned} \qquad (38)$$

appears to be the product of the following two equations

$$\lambda^3 + 2\zeta_1\omega_{n_1}\lambda^2 + \omega_{n_1}{}^2\lambda + \frac{\omega_{n_1}{}^2}{d_1} = 0 \quad \text{and} \quad \lambda^3 + 2\zeta_2\omega_{n_2}\lambda^2 + \omega_{n_2}{}^2\lambda + \frac{\omega_{n_2}{}^2}{d_2} = 0 \qquad (39)$$

Equations (39) are apparently of the form of Equation (33), which is the characteristic equation for the case of one vessel trying to move in the commanded path.

The characteristic equation of A then becomes

$$(\lambda^3 + 2\xi_1\omega_{n_1}\lambda^2 + \omega_{n_1}{}^2\lambda + \frac{\omega_{n_1}{}^2}{d_1}) \cdot (\lambda^3 + 2\xi_2\omega_{n_2}\lambda^2 + \omega_{n_2}{}^2\lambda + \frac{\omega_{n_2}{}^2}{d_2}) = 0 \qquad (40)$$

This conclusion lets us consider that the six eigenvalues of matrix A are the roots of Equations (39) (i.e., the eigenvalues for the case of the two vessels independently trying to follow the commanded path). This means that string stability is established if and only if both vessels had stability with the assumption they moved independently (not in a string, but separately), i.e.:

$$d_1 > \frac{1}{2\xi_1\omega_{n_1}}, \quad d_2 > \frac{1}{2\xi_2\omega_{n_2}} \qquad (41)$$

2. Numerical Results

To simplify the rest of the analysis, we select damping ratio ξ to be identical for both autopilots. Safe conclusions about the stability properties of the string can be extracted by the study of the eigenvalues of matrix A, which becomes

$$A = \begin{bmatrix} 0 & 1 & 0 & 0 & 0 & 0 \\ -\omega_{n_1}^{\,2} & -2\zeta\omega_{n_1} & \dfrac{-\omega_{n_1}^{\,2}}{d_1} & 0 & 0 & 0 \\ 1 & 0 & 0 & 0 & 0 & 0 \\ 0 & 0 & 0 & 0 & 1 & 0 \\ 0 & 0 & \dfrac{\omega_{n_2}^{\,2}}{d_2} & -\omega_{n_2}^{\,2} & -2\zeta\omega_{n_2} & \dfrac{-\omega_{n_2}^{\,2}}{d_2} \\ 0 & 0 & 0 & 1 & 0 & 0 \end{bmatrix} \tag{42}$$

In particular, we can determine the values of parameters ζ, ω_{n_1}, ω_{n_2}, d_1, d_2 for which eigenvalues of A have negative real parts, which means that the combined guidance and control law provides asymptotic stability. Actually, we select a damping ratio ζ and a $\dfrac{\omega_{n_2}}{\omega_{n_1}}$ ratio for the controllers, while natural frequency ω_{n_1} varies in a suitable range. Using the simulation code in Appendix A, we determine, for each value of $\omega_{n_1}, \omega_{n_2}$, the minimum ahead distances d_1^{sim}, d_2^{sim} for which string stability is established.

Table 1 in Appendix B summarizes the results for different damping ratios and natural frequencies. The code has run using the following values for the parameters:

1. Damping ratio ζ : min value 0.4, max 1.2, step 0.2
2. Natural frequency ω_{n_1} :min value 1,max 4.5, step 0.1
3. Ratio $\dfrac{\omega_{n_1}}{\omega_{n_2}}$: 0.5, 1 or 1.5

4. Distances d_1^{sim}, d_2^{sim}: min value 0.05, max 2, step 0.01

Distances d_1^*, d_2^* in the table are the hypothetical critical distances if each vessel moved alone and not both in a string, and are to be compared with d_1^{sim}, d_2^{sim}. From Equation (34), they are

$$d_1^* = \frac{1}{2\zeta\omega_{n_1}} \quad \text{and} \quad d_2^* = \frac{1}{2\zeta\omega_{n_2}} \tag{43}$$

As can be seen from the results, hypothetical critical distances d_1^* and d_2^* are almost the same with the minimum ahead distances d_1^{sim}, d_2^{sim} (the difference is due to the step of 0.01 in variation of d_1^{sim}, d_2^{sim}). Thus, we conclude again that the critical distances for string stability are those ones as the vessels move independently and not in a string. Therefore, we can study the stability properties of the string by studying the stability of each vessel separately.

3. Effect of Damping Ratio ζ and Natural Frequency ω_n on Stability

A quick look at stability of the system is depicted in Figures 9, 10, and 11, where nine families of curves d_2 versus d_1 were plotted for natural frequencies $\omega_{n_1} = 1$ to $\omega_{n_1} = 4.5$ with step *0.5*. The first three families are for $\frac{\omega_{n_2}}{\omega_{n_1}} = 0.5$, the next three for $\frac{\omega_{n_2}}{\omega_{n_1}} = 1$, and the last three for $\frac{\omega_{n_2}}{\omega_{n_1}} = 1.5$. The damping ratio ζ takes the values 0.6, 0.8, and 1.2.

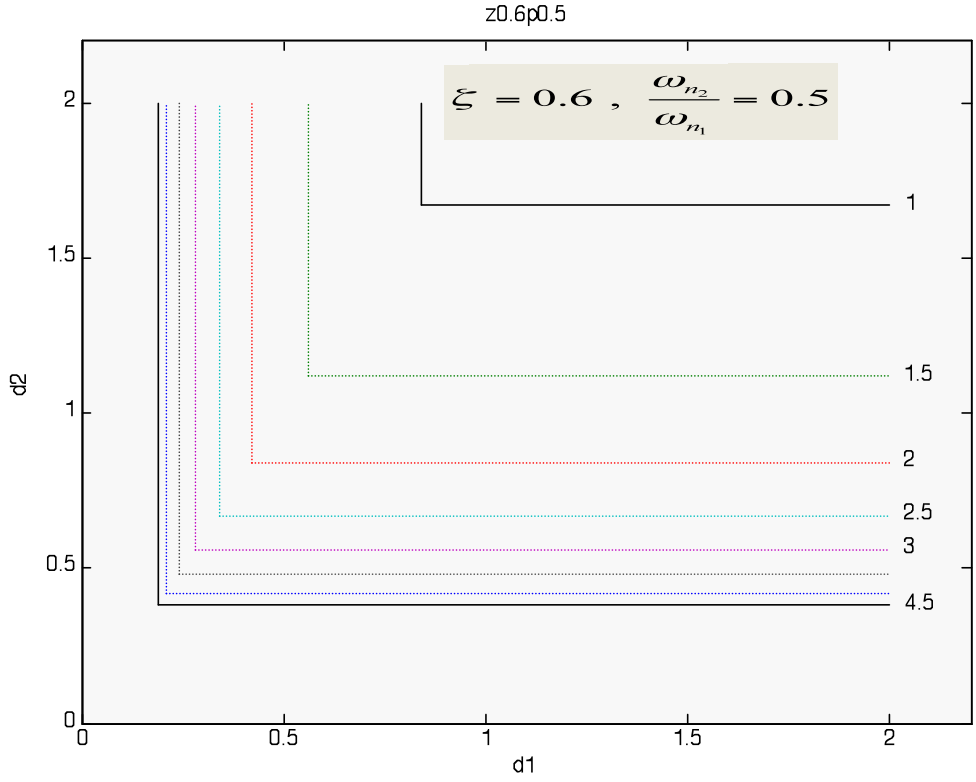
z0.6p0.5
$\xi = 0.6$, $\frac{\omega_{n_2}}{\omega_{n_1}} = 0.5$
1
1.5
2
2.5
3
4.5
d2
d1
0
0.5
1
1.5
2

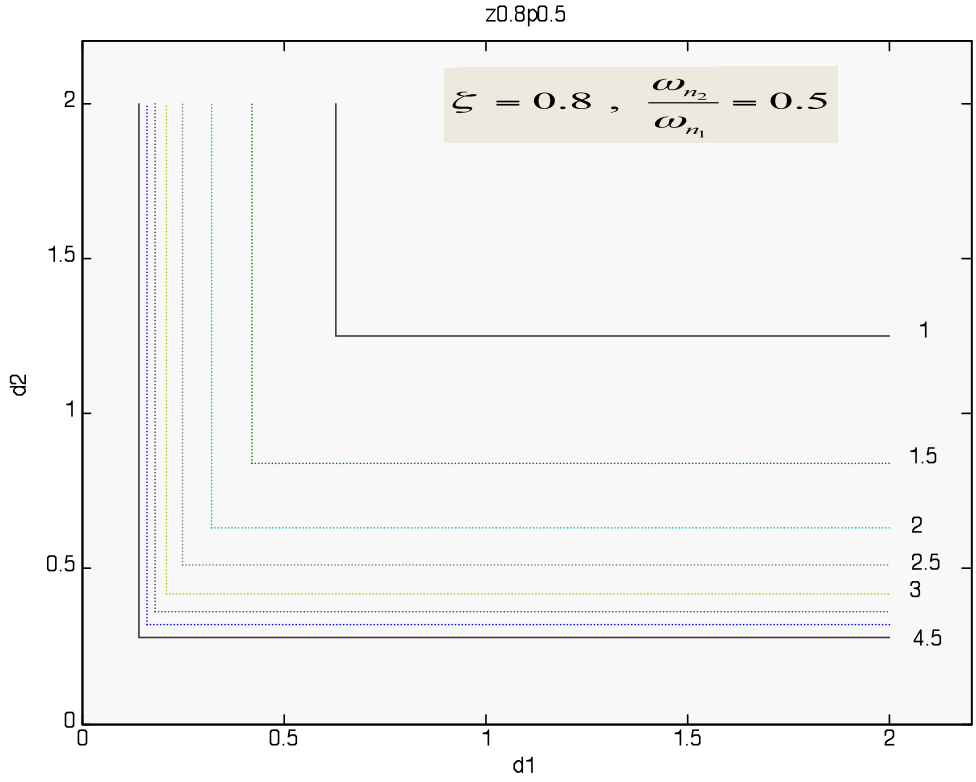
z0.8p0.5
$\xi = 0.8$, $\frac{\omega_{n_2}}{\omega_{n_1}} = 0.5$
1
1.5
2
2.5
3
4.5
d2
d1
0
0.5
1
1.5
2

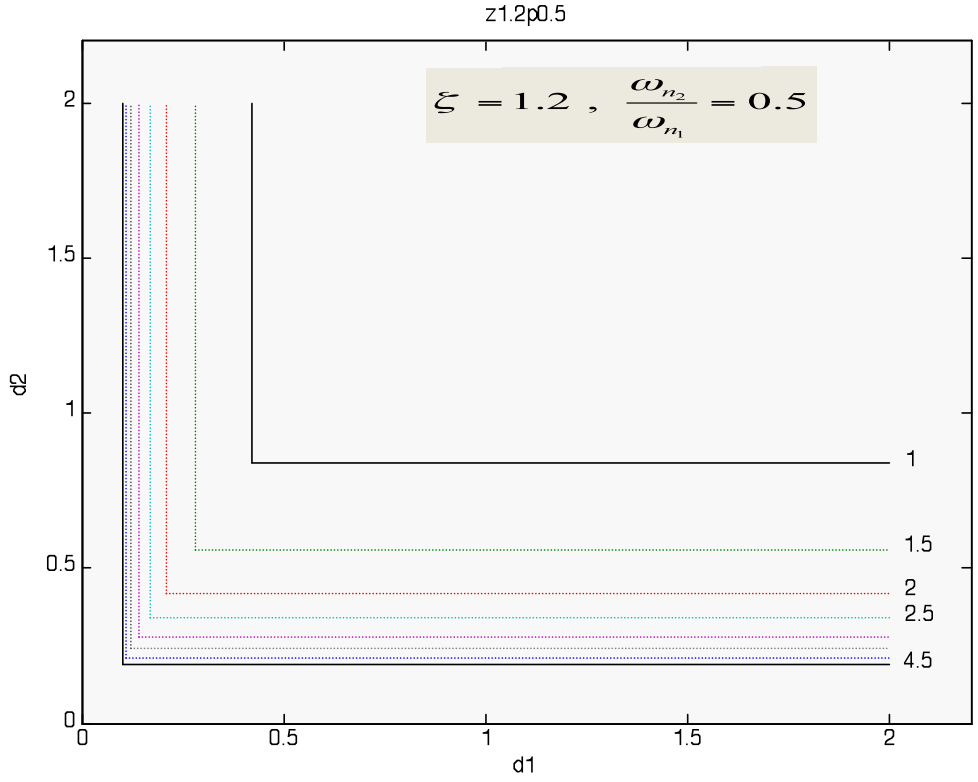

Figure 9. Three stability diagrams for $\omega_{n_2} = 0.5\omega_{n_1}$ and $\zeta = 0.6$, $\zeta = 0.8$, $\zeta = 1.2$ respectively. Stability curves are drawn for $\omega_{n_1} = 1$ to 4.5 with step 0.5

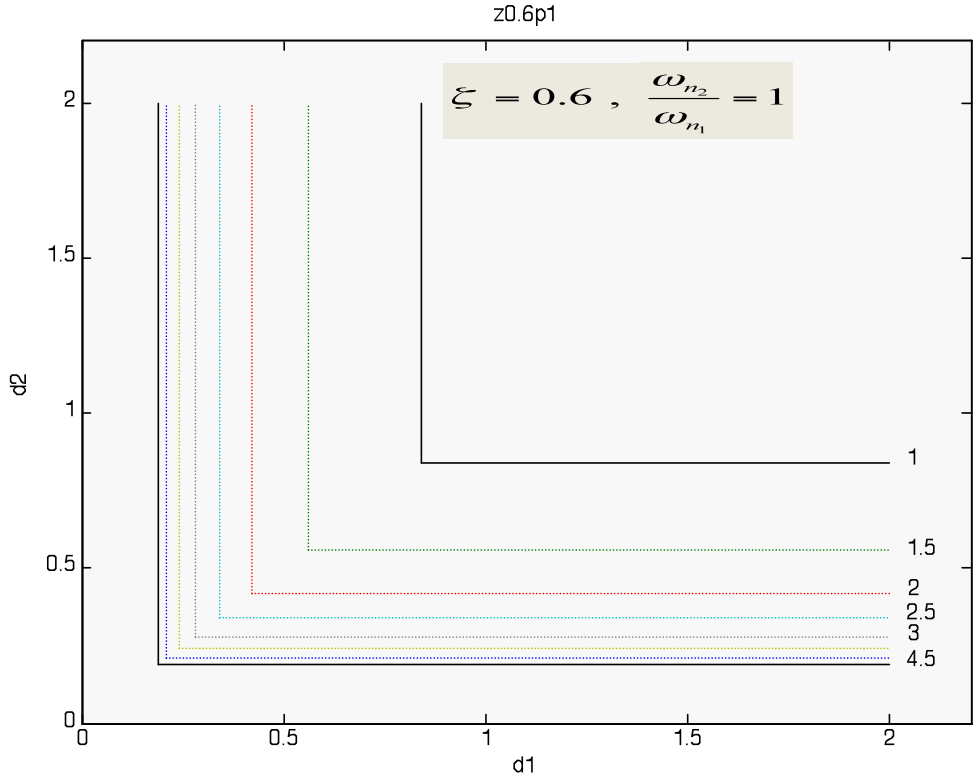
z0.6p1
$\xi = 0.6$, $\frac{\omega_{n_2}}{\omega_{n_1}} = 1$
d2
d1
0
0.5
1
1.5
2
1
1.5
2
2.5
3
4.5

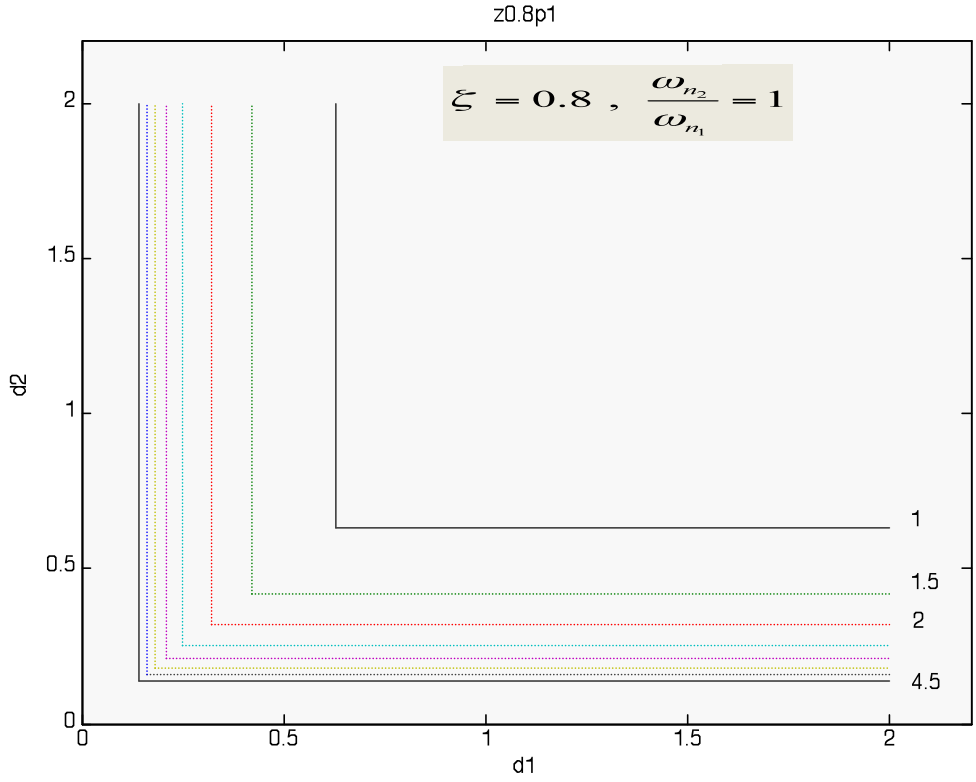
z0.8p1
$\xi = 0.8$, $\frac{\omega_{n_2}}{\omega_{n_1}} = 1$
d2
d1
0
0.5
1
1.5
2
1
1.5
2
4.5

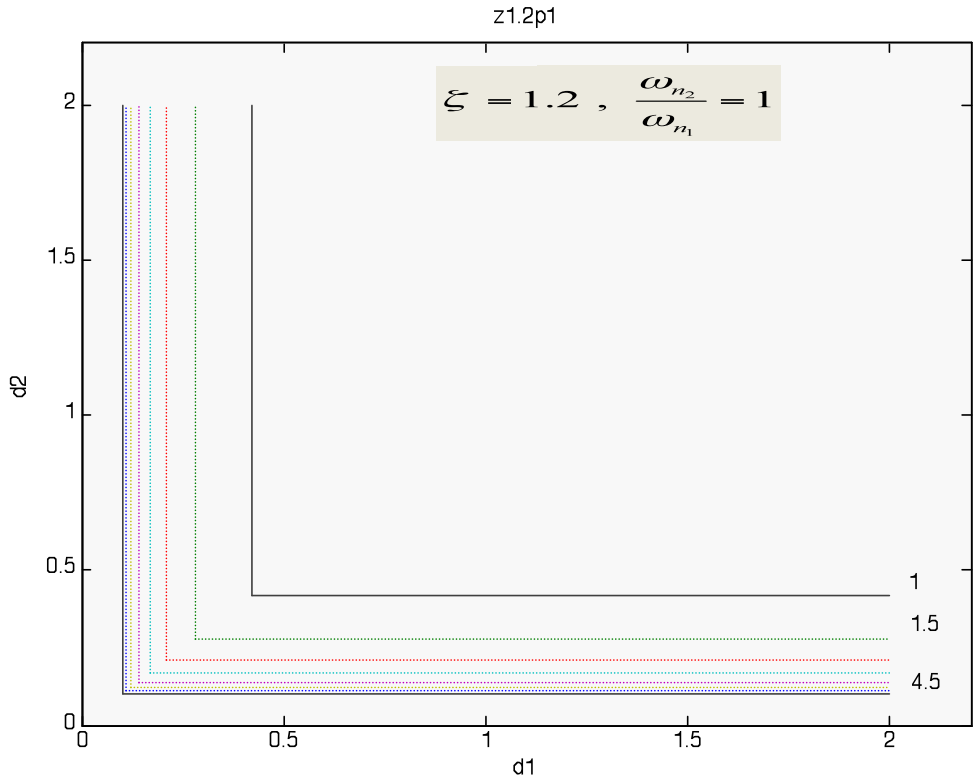

Figure 10. Three stability diagrams for $\omega_{n_2} = \omega_{n_1}$ and $\xi = 0.6$, $\xi = 0.8$, $\xi = 1.2$ respectively. Stability curves are drawn for $\omega_{n_1} = 1$ to 4.5 with step 0.5

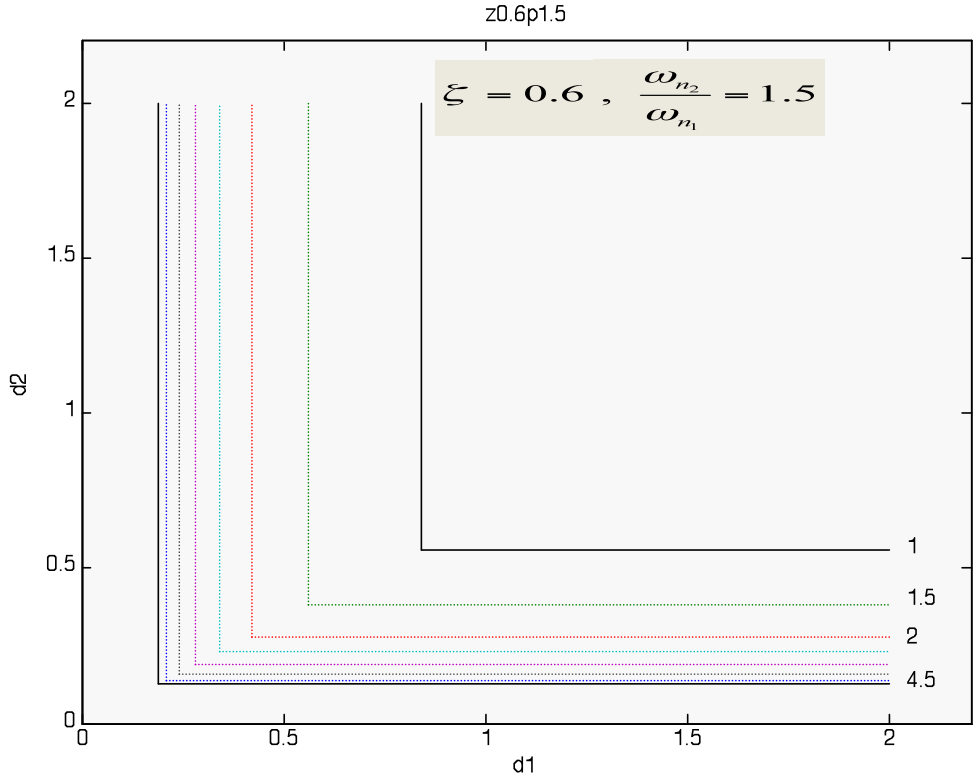
z0.6p1.5
$\xi = 0.6\ ,\ \frac{\omega_{n_2}}{\omega_{n_1}} = 1.5$
d2
d1
0
0.5
1
1.5
2
1
1.5
2
4.5

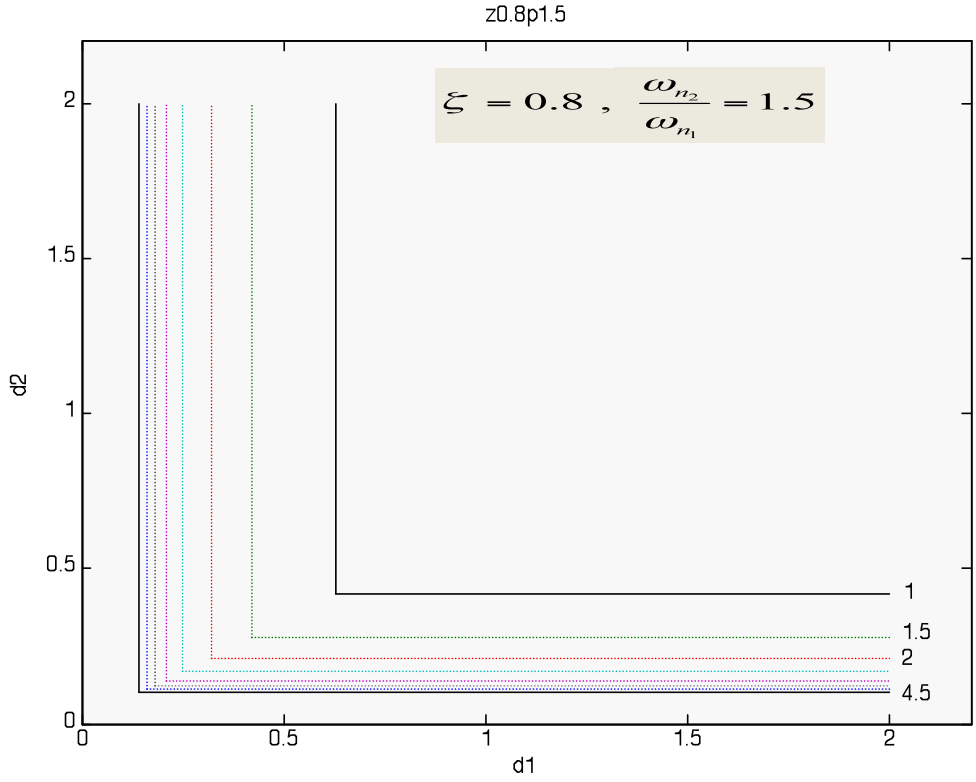
z0.8p1.5
$\xi = 0.8\ ,\ \frac{\omega_{n_2}}{\omega_{n_1}} = 1.5$
d2
d1
0
0.5
1
1.5
2
1
1.5
2
4.5

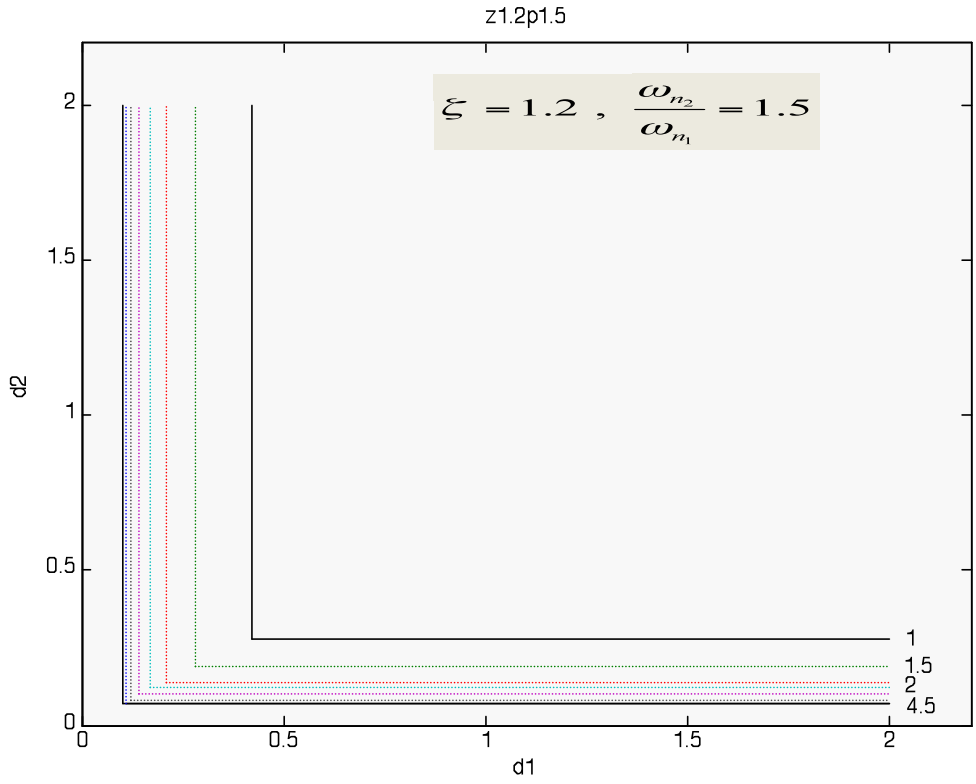

Figure 11. Three stability diagrams for $\omega_{n_2} = 1.5\omega_{n_1}$ and $\zeta = 0.6$, $\zeta = 0.8$, $\zeta = 1.2$ respectively. Stability curves are drawn for $\omega_{n_1} = 1$ to 4.5 with step 0.5

By studying the previous diagrams, we come to one basic conclusion: that, as natural frequency ω_n, damping ratio ζ ,or both are increased, the stability area expands to lower values of d_1 and d_2. We also observe that for values of natural frequency ω_{n_1} higher than three, the stability curves approach each other, and thus stability area is not affected significantly for higher values of ω_{n_1}.

Figures 12 and 13 present stability area of each vessel separately. Two families of curves for the first and the second vessel, respectively (the second vessel follows

the first one in the string), for different damping ratios from 0.4 to 1.2 and step 0.2, have been made. Natural frequency ω_{n_1} varies in the range 1-4.5 and ω_{n_2} in the range 0.5-2.25 ($\omega_{n_2} = 0.5\omega_{n_1}$). Figures 14 and 15 present another family of curves for the second vessel for the cases that $\omega_{n_2} = \omega_{n_1}$ and $\omega_{n_2} = 1.5\omega_{n_1}$, respectively.

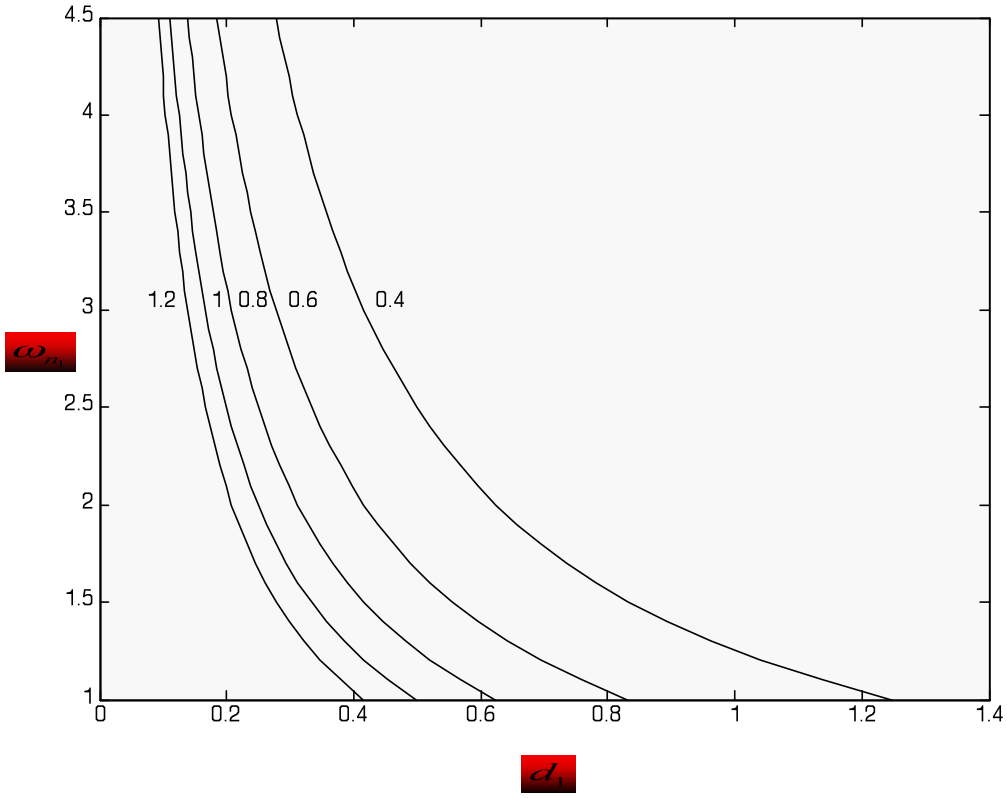

Figure 12. A family of curves for the first vessel for different damping ratios from 0.4 to 1.2 and step 0.2. Natural frequency ω_{n_1} varies in the range 1-4.5

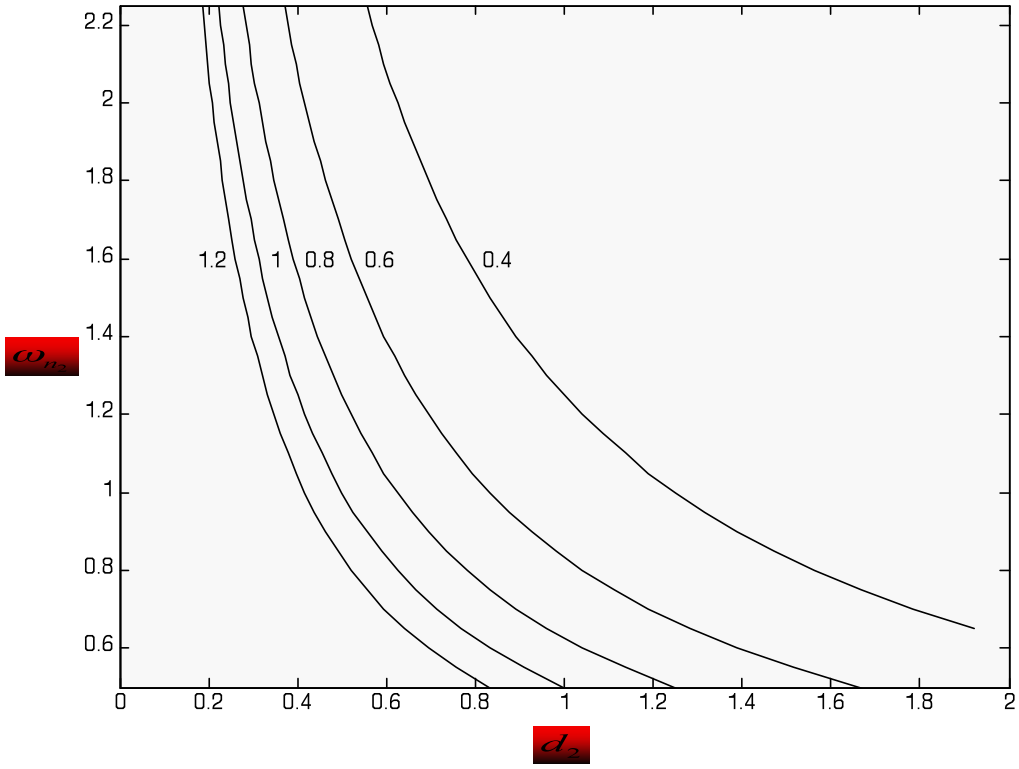

Figure 13. A family of curves for the second vessel for different damping ratios from 0.4 to 1.2 and step 0.2. Natural frequency ω_{n_1} varies in the range 1-4.5 and ω_{n_2} in the range 0.5-2.25 ($\omega_{n_2} = 0.5\omega_{n_1}$).

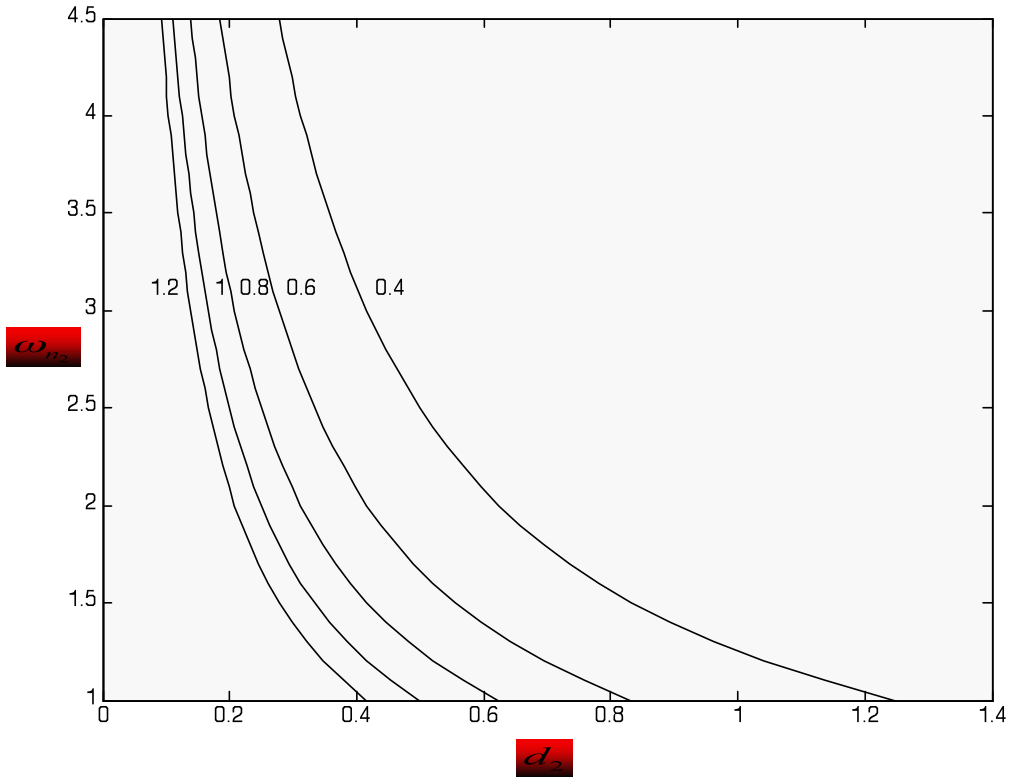

Figure 14. A family of curves for the second vessel for different damping ratios from 0.4 to 1.2 and step 0.2. Natural frequency ω_{n_1} varies in the range 1-4.5 and ω_{n_2} in the range 1-4.5 ($\omega_{n_2} = \omega_{n_1}$).

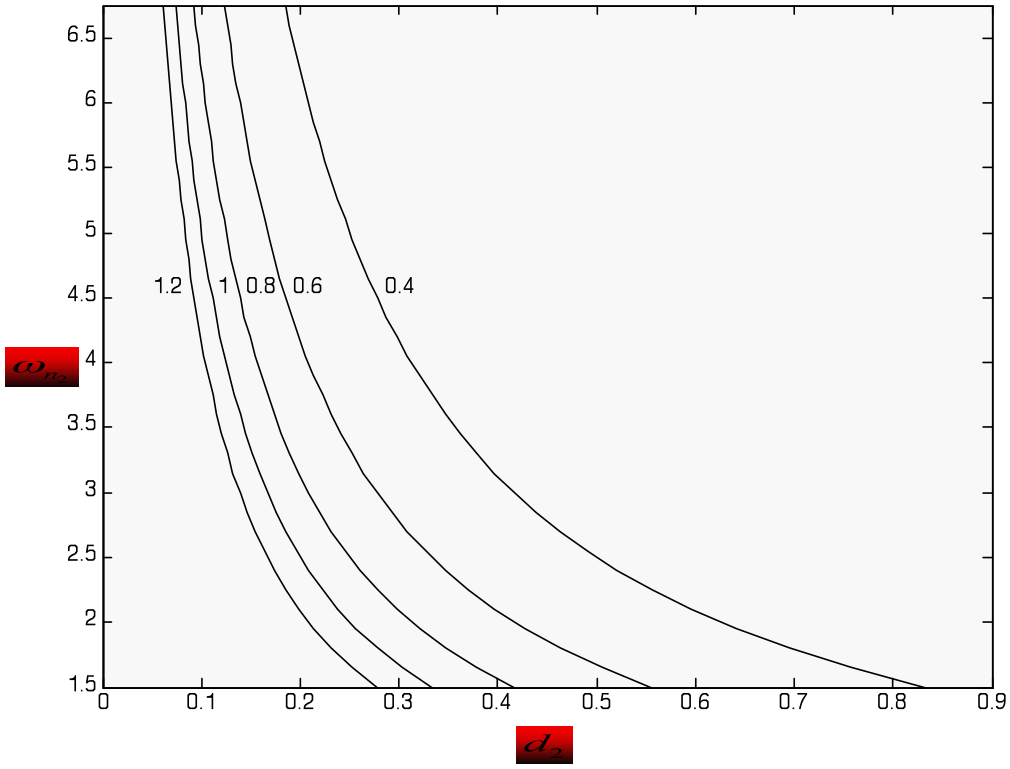

Figure 15. A family of curves for the second vessel for different damping ratios from 0.4 to 1.2 and step 0.2. Natural frequency ω_{n_1} varies in the range 1-4.5 and ω_{n_2} in the range 1.5-6.75 ($\omega_{n_2} = 1.5\omega_{n_1}$).

Again, it is noticed that the stability area increases for higher values of ζ and $\omega_{n_1}, \omega_{n_2}$. We also see that as natural frequency ω_n increases, the stability curves approach each other, and thus stability area is not affected significantly for considerably high values of ω_n.

4. Eigenvalues

For every $d_1 > d_1^*$ and $d_2 > d_2^*$, the system is stable and the vessels will follow the commanded path. The combined guidance and control law provides asymptotic stability and eigenvalues of matrix A (Equation (36)) have negative real parts. In the case that one at least of d_1 and d_2 is smaller than the minimum values, the system becomes unstable and the vessel (or vessels) moves with an oscillatory motion as a result of a complex conjugate pair of eigenvalues with positive real parts that appears in this case. At the limit of stability, some eigenvalues have zero real parts and are imaginary numbers.

As the distance d_1 approaches $d_1^* = \frac{1}{2\xi\omega_{n_1}}$ (43) (from lower and higher values), one pair of complex eigenvalues with positive imaginary parts approaches each other. Exactly when $d_1 = d_1^*$, the eigenvalues cross the imaginary axis at the same point. The eigenvalues are $\omega_{n_1} i$. Another pair of eigenvalues with the opposite imaginary parts behaves in the same way. These eigenvalues are $-\omega_{n_1} i$ on the limit. The same happens for the second vessel. Its eigenvalues will be $\pm\omega_{n_2} i$.

The last two columns of Table 1 in Appendix A show these eigenvalues at the limit of stability when $d_1 = d_1^*$ and $d_2 = d_2^*$. These values are calculated with a simulation code and it is shown that they are exactly the same with $\pm\omega_{n_1} i$, $\pm\omega_{n_2} i$.

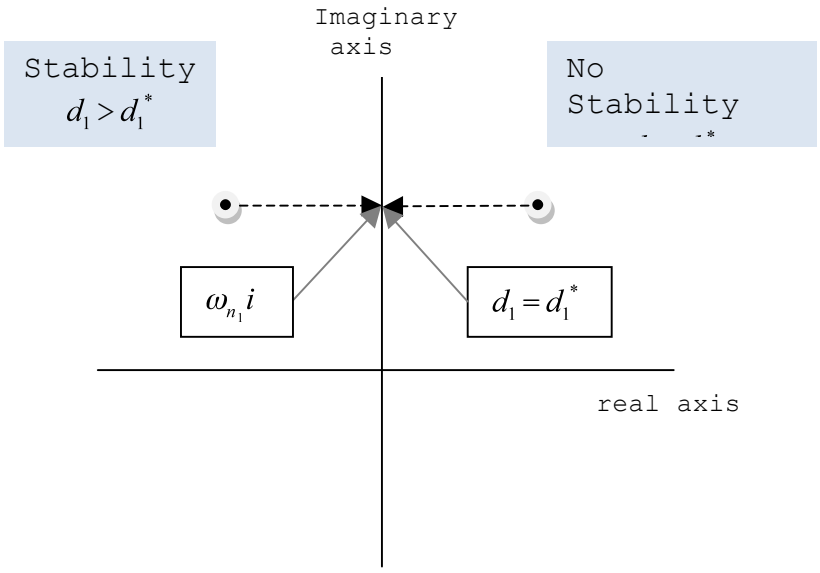

Figure 16. Change of eigenvalues as $d_1 \to d_1^*$

It is also derived from the simulation that the other two eigenvalues (matrix A has six eigenvalues) are

$$\lambda_5 = -2\zeta\omega_{n_1}\,,\ \lambda_6 = -2\zeta\omega_{n_2} \tag{44}$$

Concluding, the eigenvalues of matrix A are

$$\lambda_{1,2} = \pm\omega_{n_1} i\,,\ \lambda_{3,4} = \pm\omega_{n_2} i\,,\ \lambda_5 = -2\zeta\omega_{n_1}\,,\ \lambda_6 = -2\zeta\omega_{n_2} \tag{45}$$

5. Simulation

The following are simulation plots in Simulink. Change of deviation y_1, y_2 from the commanded path, with time, has been plotted for stability conditions ($d_1 > d_1^*$ and $d_2 > d_2^*$). The plots are for different initial conditions. Initial conditions other than the trivial solution *(ψ=r=y=0)* mainly come from external disturbances that cannot be controlled.

Simulation indicates that, under stability conditions ($d_1 > d_1^*$ and $d_2 > d_2^*$), both vessels always come back to the commanded path after a brief oscillation, and string stability is maintained.

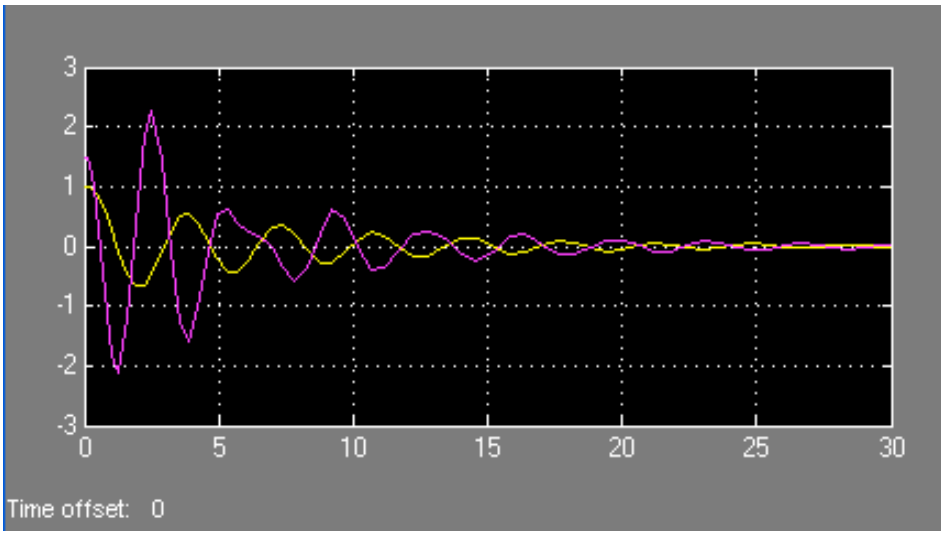

Figure 17. Change of deviation y_1, y_2 from the commanded path with time for stability conditions (I.C. $y_1 = 1$, $y_2 = 1.5$)

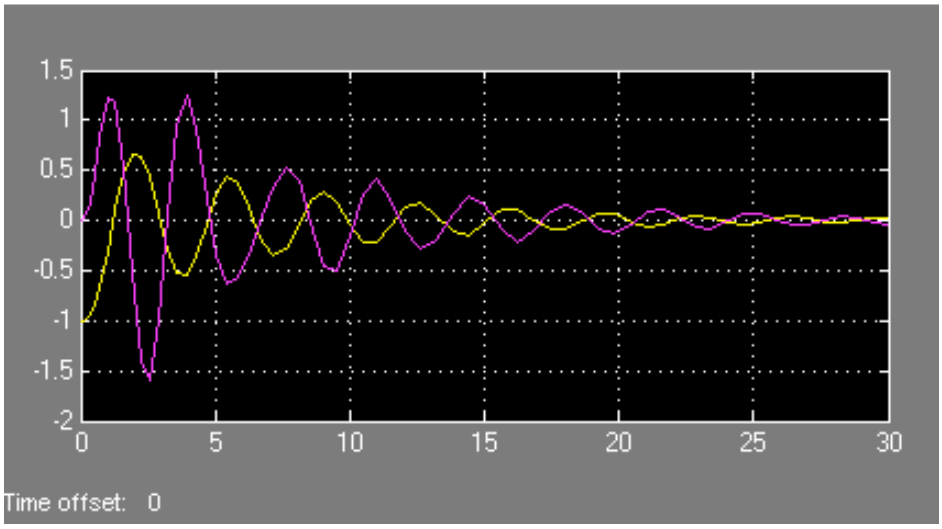

Figure 18. Change of deviation y_1, y_2 from the commanded path with time for stability conditions (I.C. $y_1 = -1$, $y_2 = 0$)

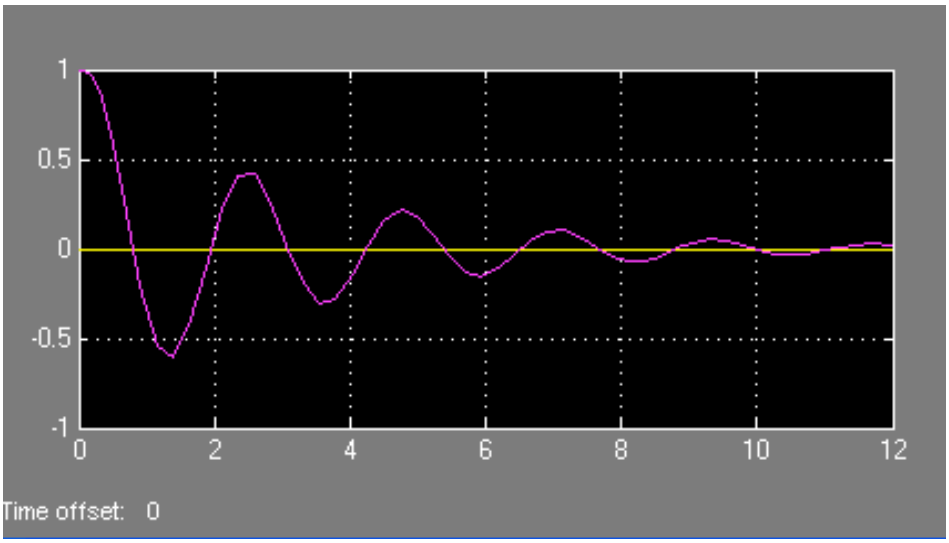

Figure 19. Change of deviation y_1, y_2 from the commanded path with time for stability conditions (I.C. $y_1 = 0$, $y_2 = 1$)

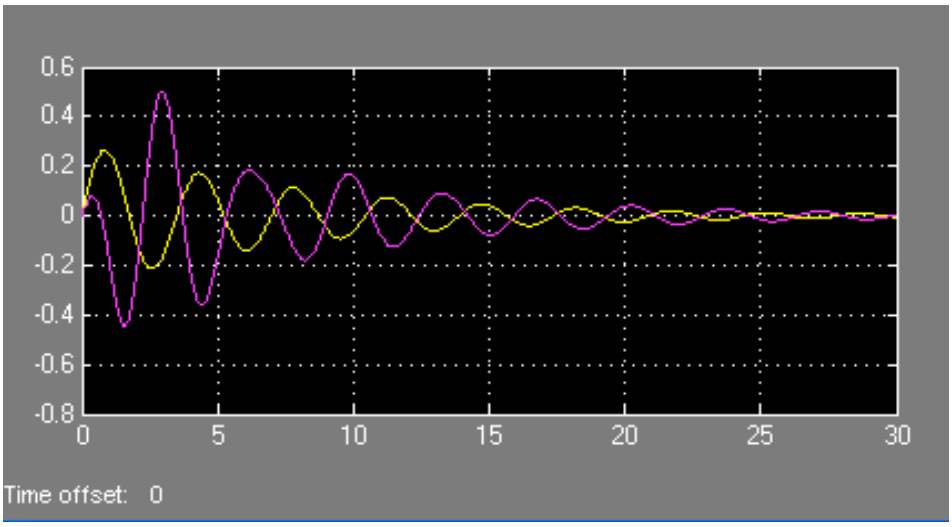

Figure 20. Change of deviation y_1, y_2 from the commanded path with time for stability conditions (I.C. $\psi_1 = 0.5$, $\psi_2 = 0.3$)

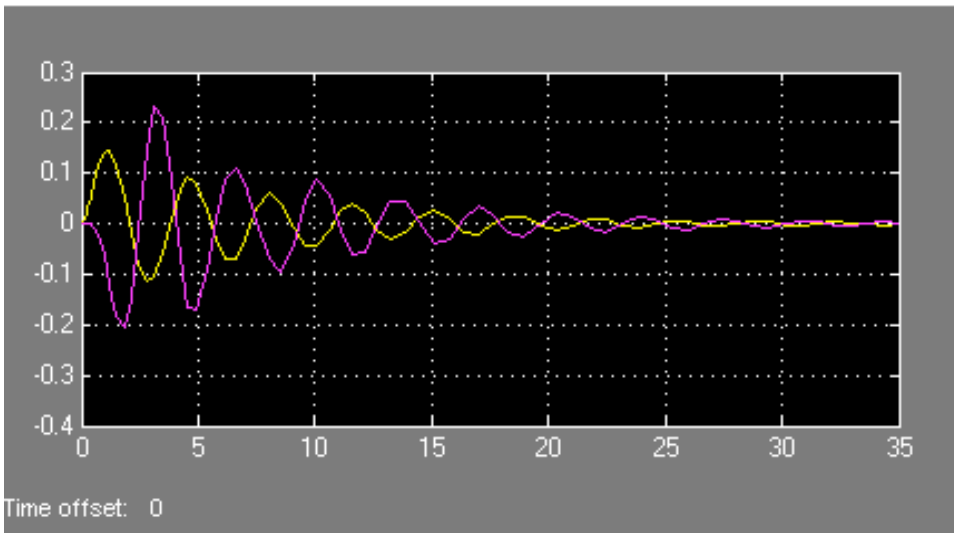

Figure 21. Change of deviation y_1, y_2 from the commanded path with time for stability conditions (I.C. $r_1 = 1$)

IV. CONCLUSIONS

This research considered the problem of path keeping of marine surface vessels along commanded paths. Especially, the phenomenon of string instability, in the case of two vessels moving in a platoon, was studied.

The following objectives have been accomplished:

a) The architecture of a path control system has been introduced.

b) An autopilot control law in coordination with a guidance law has been proposed.

c) A stability analysis has been performed.

d) The conditions for the phenomenon of string instability to be exhibited have been stated. Moreover, the question of how it can be prevented is answered.

e) A simulation was performed and verified that under stability conditions, both vessels always keep themselves at the commanded path and string stability is maintained.

Also, stability analysis has resulted in the following conclusions:

a) String stability is established if and only if both vessels had stability when they moved independently (not in a string but separately), and the critical distances for string stability are those ones as when the vessels move independently, i.e.:

$$d_1 > \frac{1}{2\zeta_1 \omega_{n_1}}, \quad d_2 > \frac{1}{2\zeta_2 \omega_{n_2}} \tag{41}$$

b) As in the case of one vessel, stability area expands to lower values of d_1 and d_2 as natural frequency ω_n, damping ratio ζ, or both are increased. Moreover, for values of natural frequency ω_{n_1} higher than three, the stability curves approach each other, and thus, stability area is not affected significantly for higher values of ω_{n_1}.

c) The six eigenvalues of matrix A in Equation (32) are the roots of Equations (39) (i.e., the eigenvalues for the case that the two vessels move independently trying to follow the commanded path). These values are

$$\lambda_{1,2} = \pm\omega_{n_1} i \text{ , } \lambda_{3,4} = \pm\omega_{n_2} i \quad \lambda_5 = -2\zeta\omega_{n_1} \text{ , } \lambda_6 = -2\zeta\omega_{n_2} \tag{45}$$

Finally, the main recommendation for future research is as follows:

a) The stability conclusions of this work are with regards to an initial stability or linear stability. It remains to be seen whether the primary mechanism of loss of stability, in the form of bifurcations to periodic solutions, is affected by the presence of multiple vehicles and their characteristics.

APPENDIX A

```
%%%%%%%%%% simulation code for string stability  area and plots
%%%%%%%%%%
%%%%%%%%%%%%%%%%%%%%%%%%%%%%%%%%%%%%%%%%%%%%%%%%%%%%%%%%%%%%%%%%
%%%%%%%%%%%%%%%%
% Christos Angelopoulos
% NPS Monterey CA - June 2011

clear
z=0.4;                      %damping ratio
p=1;                        %wn2=p*wn1
V=[];D2no_st=[];D1no_st=[];Wn1no_st=[];D2st=[];D1st=[];Wn1st=[];Wn2st=[
];
Wn2no_st=[];

%calculation of stability  area
for wn1=1:0.1:4.5           %natural frequency
    wn2=p*wn1;              %natural frequency
for d1=0.05:0.01:2
for d2=0.05:0.01:2
    A=[0 1 0 0 0 0;-wn1*wn1 -2*z*wn1 -(wn1*wn1)/d1 0 0 0;1 0 0 0 0 0;0
0 0 0 1 0;0 0 (wn2*wn2)/d2 -wn2*wn2 -2*z*wn2 -wn2*wn2/d2;0 0 0 1 0 0];
                            %system matrix A
    eigA=eig(A);
    V=[V max(real(eigA))];k=length(V);
    if V(k)>0               %no stability case
     D2no_st=[D2no_st;d2];
     D1no_st=[D1no_st;d1];
     Wn1no_st=[Wn1no_st;wn1];
     Wn2no_st=[Wn2no_st;wn2];
    else                    % stability case
     D2st=[D2st;d2];
     D1st=[D1st;d1];
     Wn1st=[Wn1st;wn1];
     Wn2st=[Wn2st;wn2];
    end
end
end
end
Wn1=[Wn1st(1) 1];
for i=1:length(Wn1st)-1
    if Wn1st(i)<Wn1st(i+1)
       Wn1=[Wn1;Wn1st(i+1) i+1];  %matrix of wn1 and position inside
Wn1st when wn1 change
    if Wn1st(i)>Wn1st(i+1)
       Wn1=[Wn1;Wn1st(i+1) i+1];
    else
    end
    end
end
D1=[];D2=[];
Wn2=[Wn1(:,1)*p Wn1(:,2)];
```

```
index=Wn2(:,2);
for j=1:length(index);
D1=[D1 D1st(index(j))];       %matrix of d1 inside D1st when wn change
D2=[D2 D2st(index(j))];
end
%Results are Wn1,Wn2,D1,D2,

%diagrams
dio=2.*ones(1,length(D1));

d1plot=[D1;dio];
d2plot=[D2;D2];
d1plot1=[D1;D1];
d2plot1=[D2;dio];
plot(d1plot,d2plot,d1plot1,d2plot1)
xlabel('d1')
ylabel('d2')
axis([0 2.2 0 2.2])

Z=[];
for q=1:length(Wn1)
    Z=[Z;z];
end
d1one_vessel=1./(2.*Z.*Wn1(:,1));
d2one_vessel=1./(2.*Z.*Wn2(:,1));
stability_matrix=[Z Wn1(:,1) Wn2(:,1) D1' D2' d1one_vessel
d2one_vessel]
                                  %final stability matrix
```

APPENDIX B

Table 1. Numerical results for: ζ 0.4 to 1.2, step 0.2. ω_{n_1} 1 to 4.5, step 0.1. d_1, d_2 0.05 to 2, step 0.01. $\frac{\omega_{n_1}}{\omega_{n_2}}$: 0.5, 1 or 1.5

ζ	ω_{n_1}	ω_{n_2}	d_1^{sim}	d_2^{sim}	d_1^*	d_2^*	*eigenvalues*	
0.4	1.3	0.65	0.97	1.93	0.961538	1.923077	± 1.3	± 0.65
0.4	1.4	0.7	0.9	1.79	0.892857	1.785714	± 1.4	± 0.7
0.4	1.5	0.75	0.84	1.67	0.833333	1.666667	± 1.5	± 0.75
0.4	1.6	0.8	0.79	1.57	0.78125	1.5625	± 1.6	± 0.8
0.4	1.7	0.85	0.74	1.48	0.735294	1.470588	± 1.7	± 0.85
0.4	1.8	0.9	0.7	1.39	0.694444	1.388889	± 1.8	± 0.9
0.4	1.9	0.95	0.66	1.32	0.657895	1.315789	± 1.9	± 0.95
0.4	2	1	0.63	1.26	0.625	1.25	± 2	± 1
0.4	2.1	1.05	0.6	1.2	0.595238	1.190476	± 2.1	± 1.05
0.4	2.2	1.1	0.57	1.14	0.568182	1.136364	± 2.2	± 1.1
0.4	2.3	1.15	0.55	1.09	0.543478	1.086957	± 2.3	± 1.15
0.4	2.4	1.2	0.53	1.05	0.520833	1.041667	± 2.4	± 1.2
0.4	2.5	1.25	0.5	1.03	0.5	1	± 2.5	± 1.25
0.4	2.6	1.3	0.49	0.97	0.480769	0.961538	± 2.6	± 1.3
0.4	2.7	1.35	0.47	0.93	0.462963	0.925926	± 2.7	± 1.35
0.4	2.8	1.4	0.45	0.9	0.446429	0.892857	± 2.8	± 1.4
0.4	2.9	1.45	0.44	0.87	0.431034	0.862069	± 2.9	± 1.45
0.4	3	1.5	0.42	0.84	0.416667	0.833333	± 3	± 1.5
0.4	3.1	1.55	0.41	0.81	0.403226	0.806452	± 3.1	± 1.55
0.4	3.2	1.6	0.4	0.79	0.390625	0.78125	± 3.2	± 1.6
0.4	3.3	1.65	0.38	0.76	0.378788	0.757576	± 3.3	± 1.65
0.4	3.4	1.7	0.37	0.74	0.367647	0.735294	± 3.4	± 1.7
0.4	3.5	1.75	0.36	0.72	0.357143	0.714286	± 3.5	± 1.75
0.4	3.6	1.8	0.35	0.7	0.347222	0.694444	± 3.6	± 1.8
0.4	3.7	1.85	0.34	0.68	0.337838	0.675676	± 3.7	± 1.85
0.4	3.8	1.9	0.33	0.66	0.328947	0.657895	± 3.8	± 1.9
0.4	3.9	1.95	0.33	0.65	0.320513	0.641026	± 3.9	± 1.95
0.4	4	2	0.32	0.63	0.3125	0.625	± 4	± 2
0.4	4.1	2.05	0.31	0.61	0.304878	0.609756	± 4.1	± 2.05

0.4	4.2	2.1	0.3	0.6	0.297619	0.595238	±	4.2	±	2.1
0.4	4.3	2.15	0.3	0.59	0.290698	0.581395	±	4.3	±	2.15
0.4	4.4	2.2	0.29	0.57	0.284091	0.568182	±	4.4	±	2.2
0.4	4.5	2.25	0.28	0.56	0.277778	0.555556	±	4.5	±	2.25

0.4	1	1	1.25	1.26	1.25	1.25	±	1	±	1
0.4	1.1	1.1	1.14	1.14	1.136364	1.136364	±	1.1	±	1.1
0.4	1.2	1.2	1.05	1.05	1.041667	1.041667	±	1.2	±	1.2
0.4	1.3	1.3	0.97	0.97	0.961538	0.961538	±	1.3	±	1.3
0.4	1.4	1.4	0.9	0.9	0.892857	0.892857	±	1.4	±	1.4
0.4	1.5	1.5	0.84	0.84	0.833333	0.833333	±	1.5	±	1.5
0.4	1.6	1.6	0.79	0.79	0.78125	0.78125	±	1.6	±	1.6
0.4	1.7	1.7	0.74	0.74	0.735294	0.735294	±	1.7	±	1.7
0.4	1.8	1.8	0.7	0.7	0.694444	0.694444	±	1.8	±	1.8
0.4	1.9	1.9	0.66	0.66	0.657895	0.657895	±	1.9	±	1.9
0.4	2	2	0.63	0.63	0.625	0.625	±	2	±	2
0.4	2.1	2.1	0.6	0.6	0.595238	0.595238	±	2.1	±	2.1
0.4	2.2	2.2	0.57	0.57	0.568182	0.568182	±	2.2	±	2.2
0.4	2.3	2.3	0.55	0.55	0.543478	0.543478	±	2.3	±	2.3
0.4	2.4	2.4	0.53	0.53	0.520833	0.520833	±	2.4	±	2.4
0.4	2.5	2.5	0.5	0.57	0.5	0.5	±	2.5	±	2.5
0.4	2.6	2.6	0.49	0.49	0.480769	0.480769	±	2.6	±	2.6
0.4	2.7	2.7	0.47	0.47	0.462963	0.462963	±	2.7	±	2.7
0.4	2.8	2.8	0.45	0.45	0.446429	0.446429	±	2.8	±	2.8
0.4	2.9	2.9	0.44	0.44	0.431034	0.431034	±	2.9	±	2.9
0.4	3	3	0.42	0.42	0.416667	0.416667	±	3	±	3
0.4	3.1	3.1	0.41	0.41	0.403226	0.403226	±	3.1	±	3.1
0.4	3.2	3.2	0.4	0.4	0.390625	0.390625	±	3.2	±	3.2
0.4	3.3	3.3	0.38	0.38	0.378788	0.378788	±	3.3	±	3.3
0.4	3.4	3.4	0.37	0.37	0.367647	0.367647	±	3.4	±	3.4
0.4	3.5	3.5	0.36	0.36	0.357143	0.357143	±	3.5	±	3.5
0.4	3.6	3.6	0.35	0.35	0.347222	0.347222	±	3.6	±	3.6
0.4	3.7	3.7	0.34	0.34	0.337838	0.337838	±	3.7	±	3.7
0.4	3.8	3.8	0.33	0.33	0.328947	0.328947	±	3.8	±	3.8
0.4	3.9	3.9	0.33	0.33	0.320513	0.320513	±	3.9	±	3.9
0.4	4	4	0.32	0.32	0.3125	0.3125	±	4	±	4
0.4	4.1	4.1	0.31	0.31	0.304878	0.304878	±	4.1	±	4.1
0.4	4.2	4.2	0.3	0.3	0.297619	0.297619	±	4.2	±	4.2
0.4	4.3	4.3	0.3	0.3	0.290698	0.290698	±	4.3	±	4.3
0.4	4.4	4.4	0.29	0.29	0.284091	0.284091	±	4.4	±	4.4
0.4	4.5	4.5	0.28	0.28	0.277778	0.277778	±	4.5	±	4.5

0.4	1	1.5	1.25	0.87	1.25	0.833333	± 1.5	± 1
0.4	1.1	1.65	1.14	0.76	1.136364	0.757576	± 1.65	± 1.1
0.4	1.2	1.8	1.05	0.7	1.041667	0.694444	± 1.8	± 1.2
0.4	1.3	1.95	0.97	0.65	0.961538	0.641026	± 1.95	± 1.3
0.4	1.4	2.1	0.9	0.6	0.892857	0.595238	± 2.1	± 1.4
0.4	1.5	2.25	0.84	0.56	0.833333	0.555556	± 2.25	± 1.5
0.4	1.6	2.4	0.79	0.53	0.78125	0.520833	± 2.4	± 1.6
0.4	1.7	2.55	0.74	0.5	0.735294	0.490196	± 2.55	± 1.7
0.4	1.8	2.7	0.7	0.47	0.694444	0.462963	± 2.7	± 1.8
0.4	1.9	2.85	0.66	0.44	0.657895	0.438596	± 2.85	± 1.9
0.4	2	3	0.63	0.42	0.625	0.416667	± 3	± 2
0.4	2.1	3.15	0.6	0.4	0.595238	0.396825	± 3.15	± 2.1
0.4	2.2	3.3	0.57	0.38	0.568182	0.378788	± 3.3	± 2.2
0.4	2.3	3.45	0.55	0.37	0.543478	0.362319	± 3.45	± 2.3
0.4	2.4	3.6	0.53	0.35	0.520833	0.347222	± 3.6	± 2.4
0.4	2.5	3.75	0.5	0.4	0.5	0.333333	± 3.75	± 2.5
0.4	2.6	3.9	0.49	0.33	0.480769	0.320513	± 3.9	± 2.6
0.4	2.7	4.05	0.47	0.31	0.462963	0.308642	± 4.05	± 2.7
0.4	2.8	4.2	0.45	0.3	0.446429	0.297619	± 4.2	± 2.8
0.4	2.9	4.35	0.44	0.29	0.431034	0.287356	± 4.35	± 2.9
0.4	3	4.5	0.42	0.28	0.416667	0.277778	± 4.5	± 3
0.4	3.1	4.65	0.41	0.27	0.403226	0.268817	± 4.65	± 3.1
0.4	3.2	4.8	0.4	0.27	0.390625	0.260417	± 4.8	± 3.2
0.4	3.3	4.95	0.38	0.26	0.378788	0.252525	± 4.95	± 3.3
0.4	3.4	5.1	0.37	0.25	0.367647	0.245098	± 5.1	± 3.4
0.4	3.5	5.25	0.36	0.24	0.357143	0.238095	± 5.25	± 3.5
0.4	3.6	5.4	0.35	0.24	0.347222	0.231481	± 5.4	± 3.6
0.4	3.7	5.55	0.34	0.23	0.337838	0.225225	± 5.55	± 3.7
0.4	3.8	5.7	0.33	0.22	0.328947	0.219298	± 5.70	± 3.8
0.4	3.9	5.85	0.33	0.22	0.320513	0.213675	± 5.85	± 3.9
0.4	4	6	0.32	0.21	0.3125	0.208333	± 6	± 4
0.4	4.1	6.15	0.31	0.21	0.304878	0.203252	± 6.15	± 4.1
0.4	4.2	6.3	0.3	0.2	0.297619	0.198413	± 6.3	± 4.2
0.4	4.3	6.45	0.3	0.2	0.290698	0.193798	± 6.45	± 4.3
0.4	4.4	6.6	0.29	0.19	0.284091	0.189394	± 6.6	± 4.4
0.4	4.5	6.75	0.28	0.19	0.277778	0.185185	± 6.75	± 4.5

0.6	1	0.5	0.84	1.67	0.833333	1.666667	± 1	± 0.5
0.6	1.1	0.55	0.76	1.52	0.757576	1.515152	± 1.1	± 0.55
0.6	1.2	0.6	0.7	1.39	0.694444	1.388889	± 1.2	± 0.6

0.6	1.3	0.65	0.65	1.29	0.641026	1.282051	± 1.3	± 0.65
0.6	1.4	0.7	0.6	1.2	0.595238	1.190476	± 1.4	± 0.7
0.6	1.5	0.75	0.56	1.12	0.555556	1.111111	± 1.5	± 0.75
0.6	1.6	0.8	0.53	1.05	0.520833	1.041667	± 1.6	± 0.8
0.6	1.7	0.85	0.5	0.99	0.490196	0.980392	± 1.7	± 0.85
0.6	1.8	0.9	0.47	0.93	0.462963	0.925926	± 1.8	± 0.9
0.6	1.9	0.95	0.44	0.88	0.438596	0.877193	± 1.9	± 0.95
0.6	2	1	0.42	0.84	0.416667	0.833333	± 2	± 1
0.6	2.1	1.05	0.4	0.8	0.396825	0.793651	± 2.1	± 1.05
0.6	2.2	1.1	0.38	0.76	0.378788	0.757576	± 2.2	± 1.1
0.6	2.3	1.15	0.37	0.73	0.362319	0.724638	± 2.3	± 1.15
0.6	2.4	1.2	0.35	0.7	0.347222	0.694444	± 2.4	± 1.2
0.6	2.5	1.25	0.34	0.67	0.333333	0.666667	± 2.5	± 1.25
0.6	2.6	1.3	0.33	0.65	0.320513	0.641026	± 2.6	± 1.3
0.6	2.7	1.35	0.31	0.62	0.308642	0.617284	± 2.7	± 1.35
0.6	2.8	1.4	0.3	0.6	0.297619	0.595238	± 2.8	± 1.4
0.6	2.9	1.45	0.29	0.58	0.287356	0.574713	± 2.9	± 1.45
0.6	3	1.5	0.28	0.56	0.277778	0.555556	± 3	± 1.5
0.6	3.1	1.55	0.27	0.54	0.268817	0.537634	± 3.1	± 1.55
0.6	3.2	1.6	0.27	0.53	0.260417	0.520833	± 3.2	± 1.6
0.6	3.3	1.65	0.26	0.51	0.252525	0.505051	± 3.3	± 1.65
0.6	3.4	1.7	0.25	0.5	0.245098	0.490196	± 3.4	± 1.7
0.6	3.5	1.75	0.24	0.48	0.238095	0.47619	± 3.5	± 1.75
0.6	3.6	1.8	0.24	0.47	0.231481	0.462963	± 3.6	± 1.8
0.6	3.7	1.85	0.23	0.46	0.225225	0.45045	± 3.7	± 1.85
0.6	3.8	1.9	0.22	0.44	0.219298	0.438596	± 3.8	± 1.9
0.6	3.9	1.95	0.22	0.43	0.213675	0.42735	± 3.9	± 1.95
0.6	4	2	0.21	0.42	0.208333	0.416667	± 4	± 2
0.6	4.1	2.05	0.21	0.41	0.203252	0.406504	± 4.1	± 2.05
0.6	4.2	2.1	0.2	0.4	0.198413	0.396825	± 4.2	± 2.1
0.6	4.3	2.15	0.2	0.39	0.193798	0.387597	± 4.3	± 2.15
0.6	4.4	2.2	0.19	0.38	0.189394	0.378788	± 4.4	± 2.2
0.6	4.5	2.25	0.19	0.38	0.185185	0.37037	± 4.5	± 2.25

0.6	1	1	0.84	0.84	0.833333	0.833333	± 1	± 1
0.6	1.1	1.1	0.76	0.76	0.757576	0.757576	± 1.1	± 1.1
0.6	1.2	1.2	0.7	0.7	0.694444	0.694444	± 1.2	± 1.2
0.6	1.3	1.3	0.65	0.65	0.641026	0.641026	± 1.3	± 1.3
0.6	1.4	1.4	0.6	0.6	0.595238	0.595238	± 1.4	± 1.4
0.6	1.5	1.5	0.56	0.56	0.555556	0.555556	± 1.5	± 1.5
0.6	1.6	1.6	0.53	0.53	0.520833	0.520833	± 1.6	± 1.6

0.6	1.7	1.7	0.5	0.5	0.490196	0.490196	± 1.7	± 1.7
0.6	1.8	1.8	0.47	0.47	0.462963	0.462963	± 1.8	± 1.8
0.6	1.9	1.9	0.44	0.44	0.438596	0.438596	± 1.9	± 1.9
0.6	2	2	0.42	0.42	0.416667	0.416667	± 2	± 2
0.6	2.1	2.1	0.4	0.4	0.396825	0.396825	± 2.1	± 2.1
0.6	2.2	2.2	0.38	0.38	0.378788	0.378788	± 2.2	± 2.2
0.6	2.3	2.3	0.37	0.37	0.362319	0.362319	± 2.3	± 2.3
0.6	2.4	2.4	0.35	0.35	0.347222	0.347222	± 2.4	± 2.4
0.6	2.5	2.5	0.34	0.34	0.333333	0.333333	± 2.5	± 2.5
0.6	2.6	2.6	0.33	0.33	0.320513	0.320513	± 2.6	± 2.6
0.6	2.7	2.7	0.31	0.31	0.308642	0.308642	± 2.7	± 2.7
0.6	2.8	2.8	0.3	0.3	0.297619	0.297619	± 2.8	± 2.8
0.6	2.9	2.9	0.29	0.29	0.287356	0.287356	± 2.9	± 2.9
0.6	3	3	0.28	0.28	0.277778	0.277778	± 3	± 3
0.6	3.1	3.1	0.27	0.27	0.268817	0.268817	± 3.1	± 3.1
0.6	3.2	3.2	0.27	0.27	0.260417	0.260417	± 3.2	± 3.2
0.6	3.3	3.3	0.26	0.26	0.252525	0.252525	± 3.3	± 3.3
0.6	3.4	3.4	0.25	0.25	0.245098	0.245098	± 3.4	± 3.4
0.6	3.5	3.5	0.24	0.24	0.238095	0.238095	± 3.5	± 3.5
0.6	3.6	3.6	0.24	0.24	0.231481	0.231481	± 3.6	± 3.6
0.6	3.7	3.7	0.23	0.23	0.225225	0.225225	± 3.7	± 3.7
0.6	3.8	3.8	0.22	0.22	0.219298	0.219298	± 3.8	± 3.8
0.6	3.9	3.9	0.22	0.22	0.213675	0.213675	± 3.9	± 3.9
0.6	4	4	0.21	0.21	0.208333	0.208333	± 4	± 4
0.6	4.1	4.1	0.21	0.21	0.203252	0.203252	± 4.1	± 4.1
0.6	4.2	4.2	0.2	0.2	0.198413	0.198413	± 4.2	± 4.2
0.6	4.3	4.3	0.2	0.2	0.193798	0.193798	± 4.3	± 4.3
0.6	4.4	4.4	0.19	0.19	0.189394	0.189394	± 4.4	± 4.4
0.6	4.5	4.5	0.19	0.19	0.185185	0.185185	± 4.5	± 4.5

0.6	1	1.5	0.84	0.56	0.833333	0.555556	± 1.5	± 1
0.6	1.1	1.65	0.76	0.51	0.757576	0.505051	± 1.65	± 1.1
0.6	1.2	1.8	0.7	0.47	0.694444	0.462963	± 1.8	± 1.2
0.6	1.3	1.95	0.65	0.43	0.641026	0.42735	± 1.95	± 1.3
0.6	1.4	2.1	0.6	0.4	0.595238	0.396825	± 2.1	± 1.4
0.6	1.5	2.25	0.56	0.38	0.555556	0.37037	± 2.25	± 1.5
0.6	1.6	2.4	0.53	0.35	0.520833	0.347222	± 2.4	± 1.6
0.6	1.7	2.55	0.5	0.33	0.490196	0.326797	± 2.55	± 1.7
0.6	1.8	2.7	0.47	0.31	0.462963	0.308642	± 2.7	± 1.8
0.6	1.9	2.85	0.44	0.3	0.438596	0.292398	± 2.85	± 1.9
0.6	2	3	0.42	0.28	0.416667	0.277778	± 3	± 2

0.6	2.1	3.15	0.4	0.27	0.396825	0.26455	± 3.15	± 2.1
0.6	2.2	3.3	0.38	0.26	0.378788	0.252525	± 3.3	± 2.2
0.6	2.3	3.45	0.37	0.25	0.362319	0.241546	± 3.45	± 2.3
0.6	2.4	3.6	0.35	0.24	0.347222	0.231481	± 3.6	± 2.4
0.6	2.5	3.75	0.34	0.23	0.333333	0.222222	± 3.75	± 2.5
0.6	2.6	3.9	0.33	0.22	0.320513	0.213675	± 3.9	± 2.6
0.6	2.7	4.05	0.31	0.21	0.308642	0.205761	± 4.05	± 2.7
0.6	2.8	4.2	0.3	0.2	0.297619	0.198413	± 4.2	± 2.8
0.6	2.9	4.35	0.29	0.2	0.287356	0.191571	± 4.35	± 2.9
0.6	3	4.5	0.28	0.19	0.277778	0.185185	± 4.5	± 3
0.6	3.1	4.65	0.27	0.18	0.268817	0.179211	± 4.65	± 3.1
0.6	3.2	4.8	0.27	0.18	0.260417	0.173611	± 4.8	± 3.2
0.6	3.3	4.95	0.26	0.17	0.252525	0.16835	± 4.95	± 3.3
0.6	3.4	5.1	0.25	0.17	0.245098	0.163399	± 5.1	± 3.4
0.6	3.5	5.25	0.24	0.16	0.238095	0.15873	± 5.25	± 3.5
0.6	3.6	5.4	0.24	0.16	0.231481	0.154321	± 5.4	± 3.6
0.6	3.7	5.55	0.23	0.16	0.225225	0.15015	± 5.55	± 3.7
0.6	3.8	5.7	0.22	0.15	0.219298	0.146199	± 5.7	± 3.8
0.6	3.9	5.85	0.22	0.15	0.213675	0.14245	± 5.85	± 3.9
0.6	4	6	0.21	0.14	0.208333	0.138889	± 6	± 4
0.6	4.1	6.15	0.21	0.14	0.203252	0.135501	± 6.15	± 4.1
0.6	4.2	6.3	0.2	0.14	0.198413	0.132275	± 6.3	± 4.2
0.6	4.3	6.45	0.2	0.13	0.193798	0.129199	± 6.45	± 4.3
0.6	4.4	6.6	0.19	0.13	0.189394	0.126263	± 6.6	± 4.4
0.6	4.5	6.75	0.19	0.13	0.185185	0.123457	± 6.75	± 4.5

0.8	1	0.5	0.63	1.25	0.625	1.25	± 1	± 0.5
0.8	1.1	0.55	0.57	1.14	0.568182	1.136364	± 1.1	± 0.55
0.8	1.2	0.6	0.53	1.05	0.520833	1.041667	± 1.2	± 0.6
0.8	1.3	0.65	0.49	0.97	0.480769	0.961538	± 1.3	± 0.65
0.8	1.4	0.7	0.45	0.9	0.446429	0.892857	± 1.4	± 0.7
0.8	1.5	0.75	0.42	0.84	0.416667	0.833333	± 1.5	± 0.75
0.8	1.6	0.8	0.4	0.79	0.390625	0.78125	± 1.6	± 0.8
0.8	1.7	0.85	0.37	0.74	0.367647	0.735294	± 1.7	± 0.85
0.8	1.8	0.9	0.35	0.7	0.347222	0.694444	± 1.8	± 0.9
0.8	1.9	0.95	0.33	0.66	0.328947	0.657895	± 1.9	± 0.95
0.8	2	1	0.32	0.63	0.3125	0.625	± 2	± 1
0.8	2.1	1.05	0.3	0.6	0.297619	0.595238	± 2.1	± 1.05
0.8	2.2	1.1	0.29	0.57	0.284091	0.568182	± 2.2	± 1.1
0.8	2.3	1.15	0.28	0.55	0.271739	0.543478	± 2.3	± 1.15
0.8	2.4	1.2	0.27	0.53	0.260417	0.520833	± 2.4	± 1.2

0.8	2.5	1.25	0.25	0.51	0.25	0.5	±	2.5	±	1.25
0.8	2.6	1.3	0.25	0.49	0.240385	0.480769	±	2.6	±	1.3
0.8	2.7	1.35	0.24	0.47	0.231481	0.462963	±	2.7	±	1.35
0.8	2.8	1.4	0.23	0.45	0.223214	0.446429	±	2.8	±	1.4
0.8	2.9	1.45	0.22	0.44	0.215517	0.431034	±	2.9	±	1.45
0.8	3	1.5	0.21	0.42	0.208333	0.416667	±	3	±	1.5
0.8	3.1	1.55	0.21	0.41	0.201613	0.403226	±	3.1	±	1.55
0.8	3.2	1.6	0.2	0.4	0.195313	0.390625	±	3.2	±	1.6
0.8	3.3	1.65	0.19	0.38	0.189394	0.378788	±	3.3	±	1.65
0.8	3.4	1.7	0.19	0.37	0.183824	0.367647	±	3.4	±	1.7
0.8	3.5	1.75	0.18	0.36	0.178571	0.357143	±	3.5	±	1.75
0.8	3.6	1.8	0.18	0.35	0.173611	0.347222	±	3.6	±	1.8
0.8	3.7	1.85	0.17	0.34	0.168919	0.337838	±	3.7	±	1.85
0.8	3.8	1.9	0.17	0.33	0.164474	0.328947	±	3.8	±	1.9
0.8	3.9	1.95	0.17	0.33	0.160256	0.320513	±	3.9	±	1.95
0.8	4	2	0.16	0.32	0.15625	0.3125	±	4	±	2
0.8	4.1	2.05	0.16	0.31	0.152439	0.304878	±	4.1	±	2.05
0.8	4.2	2.1	0.15	0.3	0.14881	0.297619	±	4.2	±	2.1
0.8	4.3	2.15	0.15	0.3	0.145349	0.290698	±	4.3	±	2.15
0.8	4.4	2.2	0.15	0.29	0.142045	0.284091	±	4.4	±	2.2
0.8	4.5	2.25	0.14	0.28	0.138889	0.277778	±	4.5	±	2.25

0.8	1	1	0.63	0.63	0.625	0.625	±	1	±	1
0.8	1.1	1.1	0.57	0.57	0.568182	0.568182	±	1.1	±	1.1
0.8	1.2	1.2	0.53	0.53	0.520833	0.520833	±	1.2	±	1.2
0.8	1.3	1.3	0.49	0.49	0.480769	0.480769	±	1.3	±	1.3
0.8	1.4	1.4	0.45	0.45	0.446429	0.446429	±	1.4	±	1.4
0.8	1.5	1.5	0.42	0.42	0.416667	0.416667	±	1.5	±	1.5
0.8	1.6	1.6	0.4	0.4	0.390625	0.390625	±	1.6	±	1.6
0.8	1.7	1.7	0.37	0.37	0.367647	0.367647	±	1.7	±	1.7
0.8	1.8	1.8	0.35	0.35	0.347222	0.347222	±	1.8	±	1.8
0.8	1.9	1.9	0.33	0.33	0.328947	0.328947	±	1.9	±	1.9
0.8	2	2	0.32	0.32	0.3125	0.3125	±	2	±	2
0.8	2.1	2.1	0.3	0.3	0.297619	0.297619	±	2.1	±	2.1
0.8	2.2	2.2	0.29	0.29	0.284091	0.284091	±	2.2	±	2.2
0.8	2.3	2.3	0.28	0.28	0.271739	0.271739	±	2.3	±	2.3
0.8	2.4	2.4	0.27	0.27	0.260417	0.260417	±	2.4	±	2.4
0.8	2.5	2.5	0.25	0.27	0.25	0.25	±	2.5	±	2.5
0.8	2.6	2.6	0.25	0.25	0.240385	0.240385	±	2.6	±	2.6
0.8	2.7	2.7	0.24	0.24	0.231481	0.231481	±	2.7	±	2.7
0.8	2.8	2.8	0.23	0.23	0.223214	0.223214	±	2.8	±	2.8

0.8	2.9	2.9	0.22	0.22	0.215517	0.215517	± 2.9	± 2.9
0.8	3	3	0.21	0.21	0.208333	0.208333	± 3	± 3
0.8	3.1	3.1	0.21	0.21	0.201613	0.201613	± 3.1	± 3.1
0.8	3.2	3.2	0.2	0.2	0.195313	0.195313	± 3.2	± 3.2
0.8	3.3	3.3	0.19	0.19	0.189394	0.189394	± 3.3	± 3.3
0.8	3.4	3.4	0.19	0.19	0.183824	0.183824	± 3.4	± 3.4
0.8	3.5	3.5	0.18	0.18	0.178571	0.178571	± 3.5	± 3.5
0.8	3.6	3.6	0.18	0.18	0.173611	0.173611	± 3.6	± 3.6
0.8	3.7	3.7	0.17	0.17	0.168919	0.168919	± 3.7	± 3.7
0.8	3.8	3.8	0.17	0.17	0.164474	0.164474	± 3.8	± 3.8
0.8	3.9	3.9	0.17	0.17	0.160256	0.160256	± 3.9	± 3.9
0.8	4	4	0.16	0.16	0.15625	0.15625	± 4	± 4
0.8	4.1	4.1	0.16	0.16	0.152439	0.152439	± 4.1	± 4.1
0.8	4.2	4.2	0.15	0.15	0.14881	0.14881	± 4.2	± 4.2
0.8	4.3	4.3	0.15	0.15	0.145349	0.145349	± 4.3	± 4.3
0.8	4.4	4.4	0.15	0.15	0.142045	0.142045	± 4.4	± 4.4
0.8	4.5	4.5	0.14	0.14	0.138889	0.138889	± 4.5	± 4.5

0.8	1	1.5	0.63	0.42	0.625	0.416667	± 1.5	± 1
0.8	1.1	1.65	0.57	0.38	0.568182	0.378788	± 1.65	± 1.1
0.8	1.2	1.8	0.53	0.35	0.520833	0.347222	± 1.8	± 1.2
0.8	1.3	1.95	0.49	0.33	0.480769	0.320513	± 1.95	± 1.3
0.8	1.4	2.1	0.45	0.3	0.446429	0.297619	± 2.1	± 1.4
0.8	1.5	2.25	0.42	0.28	0.416667	0.277778	± 2.25	± 1.5
0.8	1.6	2.4	0.4	0.27	0.390625	0.260417	± 2.4	± 1.6
0.8	1.7	2.55	0.37	0.25	0.367647	0.245098	± 1.7	± 2.55
0.8	1.8	2.7	0.35	0.24	0.347222	0.231481	± 2.7	± 1.8
0.8	1.9	2.85	0.33	0.22	0.328947	0.219298	± 2.85	± 1.9
0.8	2	3	0.32	0.21	0.3125	0.208333	± 3	± 2
0.8	2.1	3.15	0.3	0.2	0.297619	0.198413	± 3.15	± 2.1
0.8	2.2	3.3	0.29	0.19	0.284091	0.189394	± 3.3	± 2.2
0.8	2.3	3.45	0.28	0.19	0.271739	0.181159	± 3.45	± 2.3
0.8	2.4	3.6	0.27	0.18	0.260417	0.173611	± 3.6	± 2.4
0.8	2.5	3.75	0.25	0.17	0.25	0.166667	± 3.75	± 2.5
0.8	2.6	3.9	0.25	0.17	0.240385	0.160256	± 3.9	± 2.6
0.8	2.7	4.05	0.24	0.16	0.231481	0.154321	± 4.05	± 2.7
0.8	2.8	4.2	0.23	0.15	0.223214	0.14881	± 4.2	± 2.8
0.8	2.9	4.35	0.22	0.15	0.215517	0.143678	± 2.9	± 4.35
0.8	3	4.5	0.21	0.14	0.208333	0.138889	± 3	± 4.5
0.8	3.1	4.65	0.21	0.14	0.201613	0.134409	± 3.1	± 4.65
0.8	3.2	4.8	0.2	0.14	0.195313	0.130208	± 3.2	± 4.8

0.8	3.3	4.95	0.19	0.13	0.189394	0.126263	± 3.3	± 4.95
0.8	3.4	5.1	0.19	0.13	0.183824	0.122549	± 3.4	± 5.1
0.8	3.5	5.25	0.18	0.12	0.178571	0.119048	± 3.5	± 5.25
0.8	3.6	5.4	0.18	0.12	0.173611	0.115741	± 3.6	± 5.4
0.8	3.7	5.55	0.17	0.12	0.168919	0.112613	± 5.55	± 3.7
0.8	3.8	5.7	0.17	0.11	0.164474	0.109649	± 5.7	± 3.8
0.8	3.9	5.85	0.17	0.11	0.160256	0.106838	± 5.85	± 3.9
0.8	4	6	0.16	0.11	0.15625	0.104167	± 6	± 4
0.8	4.1	6.15	0.16	0.11	0.152439	0.101626	± 6.15	± 4.1
0.8	4.2	6.3	0.15	0.1	0.14881	0.099206	± 6.3	± 4.2
0.8	4.3	6.45	0.15	0.1	0.145349	0.096899	± 6.45	± 4.3
0.8	4.4	6.6	0.15	0.1	0.142045	0.094697	± 6.6	± 4.4
0.8	4.5	6.75	0.14	0.1	0.138889	0.092593	± 6.75	± 4.5

1	1	0.5	0.5	1.07	0.5	1	± 1	± 0.5
1	1.1	0.55	0.46	0.91	0.454545	0.909091	± 1.1	± 0.55
1	1.2	0.6	0.42	0.84	0.416667	0.833333	± 1.2	± 0.6
1	1.3	0.65	0.39	0.77	0.384615	0.769231	± 1.3	± 0.65
1	1.4	0.7	0.36	0.72	0.357143	0.714286	± 1.4	± 0.7
1	1.5	0.75	0.34	0.67	0.333333	0.666667	± 1.5	± 0.75
1	1.6	0.8	0.32	0.63	0.3125	0.625	± 1.6	± 0.8
1	1.7	0.85	0.3	0.59	0.294118	0.588235	± 1.7	± 0.85
1	1.8	0.9	0.28	0.56	0.277778	0.555556	± 1.8	± 0.9
1	1.9	0.95	0.27	0.53	0.263158	0.526316	± 1.9	± 0.95
1	2	1	0.25	0.54	0.25	0.5	± 2	± 1
1	2.1	1.05	0.24	0.48	0.238095	0.47619	± 2.1	± 1.05
1	2.2	1.1	0.23	0.46	0.227273	0.454545	± 2.2	± 1.1
1	2.3	1.15	0.22	0.44	0.217391	0.434783	± 2.3	± 1.15
1	2.4	1.2	0.21	0.42	0.208333	0.416667	± 2.4	± 1.2
1	2.5	1.25	0.2	0.41	0.2	0.4	± 2.5	± 1.25
1	2.6	1.3	0.2	0.39	0.192308	0.384615	± 2.6	± 1.3
1	2.7	1.35	0.19	0.38	0.185185	0.37037	± 2.7	± 1.35
1	2.8	1.4	0.18	0.36	0.178571	0.357143	± 2.8	± 1.4
1	2.9	1.45	0.18	0.35	0.172414	0.344828	± 2.9	± 1.45
1	3	1.5	0.17	0.34	0.166667	0.333333	± 3	± 1.5
1	3.1	1.55	0.17	0.33	0.16129	0.322581	± 3.1	± 1.55
1	3.2	1.6	0.16	0.32	0.15625	0.3125	± 3.2	± 1.6
1	3.3	1.65	0.16	0.31	0.151515	0.30303	± 3.3	± 1.65
1	3.4	1.7	0.15	0.3	0.147059	0.294118	± 3.4	± 1.7
1	3.5	1.75	0.15	0.29	0.142857	0.285714	± 3.5	± 1.75
1	3.6	1.8	0.14	0.28	0.138889	0.277778	± 3.6	± 1.8

1	3.7	1.85	0.14	0.28	0.135135	0.27027	±	3.7	±	1.85
1	3.8	1.9	0.14	0.27	0.131579	0.263158	±	3.8	±	1.9
1	3.9	1.95	0.13	0.26	0.128205	0.25641	±	3.9	±	1.95
1	4	2	0.13	0.25	0.125	0.25	±	4	±	2
1	4.1	2.05	0.13	0.25	0.121951	0.243902	±	4.1	±	2.05
1	4.2	2.1	0.12	0.24	0.119048	0.238095	±	4.2	±	2.1
1	4.3	2.15	0.12	0.24	0.116279	0.232558	±	4.3	±	2.15
1	4.4	2.2	0.12	0.23	0.113636	0.227273	±	4.4	±	2.2
1	4.5	2.25	0.12	0.23	0.111111	0.222222	±	4.5	±	2.25

1	1	1	0.5	0.52	0.5	0.5	±	1	±	1
1	1.1	1.1	0.46	0.46	0.454545	0.454545	±	1.1	±	1.1
1	1.2	1.2	0.42	0.42	0.416667	0.416667	±	1.2	±	1.2
1	1.3	1.3	0.39	0.39	0.384615	0.384615	±	1.3	±	1.3
1	1.4	1.4	0.36	0.36	0.357143	0.357143	±	1.4	±	1.4
1	1.5	1.5	0.34	0.34	0.333333	0.333333	±	1.5	±	1.5
1	1.6	1.6	0.32	0.32	0.3125	0.3125	±	1.6	±	1.6
1	1.7	1.7	0.3	0.3	0.294118	0.294118	±	1.7	±	1.7
1	1.8	1.8	0.28	0.28	0.277778	0.277778	±	1.8	±	1.8
1	1.9	1.9	0.27	0.27	0.263158	0.263158	±	1.9	±	1.9
1	2	2	0.25	0.26	0.25	0.25	±	2	±	2
1	2.1	2.1	0.24	0.24	0.238095	0.238095	±	2.1	±	2.1
1	2.2	2.2	0.23	0.23	0.227273	0.227273	±	2.2	±	2.2
1	2.3	2.3	0.22	0.22	0.217391	0.217391	±	2.3	±	2.3
1	2.4	2.4	0.21	0.21	0.208333	0.208333	±	2.4	±	2.4
1	2.5	2.5	0.2	0.21	0.2	0.2	±	2.5	±	2.5
1	2.6	2.6	0.2	0.2	0.192308	0.192308	±	2.6	±	2.6
1	2.7	2.7	0.19	0.19	0.185185	0.185185	±	2.7	±	2.7
1	2.8	2.8	0.18	0.18	0.178571	0.178571	±	2.8	±	2.8
1	2.9	2.9	0.18	0.18	0.172414	0.172414	±	2.9	±	2.9
1	3	3	0.17	0.17	0.166667	0.166667	±	3	±	3
1	3.1	3.1	0.17	0.17	0.16129	0.16129	±	3.1	±	3.1
1	3.2	3.2	0.16	0.16	0.15625	0.15625	±	3.2	±	3.2
1	3.3	3.3	0.16	0.16	0.151515	0.151515	±	3.3	±	3.3
1	3.4	3.4	0.15	0.15	0.147059	0.147059	±	3.4	±	3.4
1	3.5	3.5	0.15	0.15	0.142857	0.142857	±	3.5	±	3.5
1	3.6	3.6	0.14	0.14	0.138889	0.138889	±	3.6	±	3.6
1	3.7	3.7	0.14	0.14	0.135135	0.135135	±	3.7	±	3.7
1	3.8	3.8	0.14	0.14	0.131579	0.131579	±	3.8	±	3.8
1	3.9	3.9	0.13	0.13	0.128205	0.128205	±	3.9	±	3.9
1	4	4	0.13	0.13	0.125	0.125	±	4	±	4

1	4.1	4.1	0.13	0.13	0.121951	0.121951	± 4.1	± 4.1
1	4.2	4.2	0.12	0.12	0.119048	0.119048	± 4.2	± 4.2
1	4.3	4.3	0.12	0.12	0.116279	0.116279	± 4.3	± 4.3
1	4.4	4.4	0.12	0.12	0.113636	0.113636	± 4.4	± 4.4
1	4.5	4.5	0.12	0.12	0.111111	0.111111	± 4.5	± 4.5

1	1	1.5	0.5	0.35	0.5	0.333333	± 1.5	± 1
1	1.1	1.65	0.46	0.31	0.454545	0.30303	± 1.65	± 1.1
1	1.2	1.8	0.42	0.28	0.416667	0.277778	± 1.8	± 1.2
1	1.3	1.95	0.39	0.26	0.384615	0.25641	± 1.95	± 1.3
1	1.4	2.1	0.36	0.24	0.357143	0.238095	± 2.1	± 1.4
1	1.5	2.25	0.34	0.23	0.333333	0.222222	± 2.25	± 1.5
1	1.6	2.4	0.32	0.21	0.3125	0.208333	± 2.4	± 1.6
1	1.7	2.55	0.3	0.2	0.294118	0.196078	± 2.55	± 1.7
1	1.8	2.7	0.28	0.19	0.277778	0.185185	± 2.7	± 1.8
1	1.9	2.85	0.27	0.18	0.263158	0.175439	± 2.85	± 1.9
1	2	3	0.25	0.17	0.25	0.166667	± 3	± 2
1	2.1	3.15	0.24	0.16	0.238095	0.15873	± 3.15	± 2.1
1	2.2	3.3	0.23	0.16	0.227273	0.151515	± 3.3	± 2.2
1	2.3	3.45	0.22	0.15	0.217391	0.144928	± 3.45	± 2.3
1	2.4	3.6	0.21	0.14	0.208333	0.138889	± 3.6	± 2.4
1	2.5	3.75	0.2	0.14	0.2	0.133333	± 3.75	± 2.5
1	2.6	3.9	0.2	0.13	0.192308	0.128205	± 3.9	± 2.6
1	2.7	4.05	0.19	0.13	0.185185	0.123457	± 2.7	± 4.05
1	2.8	4.2	0.18	0.12	0.178571	0.119048	± 2.8	± 4.2
1	2.9	4.35	0.18	0.12	0.172414	0.114943	± 2.9	± 4.35
1	3	4.5	0.17	0.12	0.166667	0.111111	± 3	± 4.5
1	3.1	4.65	0.17	0.11	0.16129	0.107527	± 3.1	± 4.65
1	3.2	4.8	0.16	0.11	0.15625	0.104167	± 4.8	± 3.2
1	3.3	4.95	0.16	0.11	0.151515	0.10101	± 3.3	± 4.95
1	3.4	5.1	0.15	0.1	0.147059	0.098039	± 5.1	± 3.4
1	3.5	5.25	0.15	0.1	0.142857	0.095238	± 5.25	± 3.5
1	3.6	5.4	0.14	0.1	0.138889	0.092593	± 5.4	± 3.6
1	3.7	5.55	0.14	0.1	0.135135	0.09009	± 5.55	± 3.7
1	3.8	5.7	0.14	0.1	0.131579	0.087719	± 5.7	± 3.8
1	3.9	5.85	0.13	0.1	0.128205	0.08547	± 5.85	± 3.9
1	4	6	0.13	0.1	0.125	0.083333	± 6	± 4
1	4.1	6.15	0.13	0.1	0.121951	0.081301	± 6.15	± 4.1
1	4.2	6.3	0.12	0.1	0.119048	0.079365	± 4.2	± 6.3
1	4.3	6.45	0.12	0.1	0.116279	0.077519	± 6.45	± 4.3
1	4.4	6.6	0.12	0.1	0.113636	0.075758	± 6.6	± 4.4

1	4.5	6.75	0.12	0.1	0.111111	0.074074	± 6.75	± 4.5

1.2	1	0.5	0.42	0.84	0.416667	0.833333	± 1	± 0.5
1.2	1.1	0.55	0.38	0.76	0.378788	0.757576	± 1.1	± 0.55
1.2	1.2	0.6	0.35	0.7	0.347222	0.694444	± 1.2	± 0.6
1.2	1.3	0.65	0.33	0.65	0.320513	0.641026	± 1.3	± 0.65
1.2	1.4	0.7	0.3	0.6	0.297619	0.595238	± 1.4	± 0.7
1.2	1.5	0.75	0.28	0.56	0.277778	0.555556	± 1.5	± 0.75
1.2	1.6	0.8	0.27	0.53	0.260417	0.520833	± 1.6	± 0.8
1.2	1.7	0.85	0.25	0.5	0.245098	0.490196	± 1.7	± 0.85
1.2	1.8	0.9	0.24	0.47	0.231481	0.462963	± 1.8	± 0.9
1.2	1.9	0.95	0.22	0.44	0.219298	0.438596	± 1.9	± 0.95
1.2	2	1	0.21	0.42	0.208333	0.416667	± 2	± 1
1.2	2.1	1.05	0.2	0.4	0.198413	0.396825	± 2.1	± 1.05
1.2	2.2	1.1	0.19	0.38	0.189394	0.378788	± 2.2	± 1.1
1.2	2.3	1.15	0.19	0.37	0.181159	0.362319	± 2.3	± 1.15
1.2	2.4	1.2	0.18	0.35	0.173611	0.347222	± 2.4	± 1.2
1.2	2.5	1.25	0.17	0.34	0.166667	0.333333	± 2.5	± 1.25
1.2	2.6	1.3	0.17	0.33	0.160256	0.320513	± 2.6	± 1.3
1.2	2.7	1.35	0.16	0.31	0.154321	0.308642	± 2.7	± 1.35
1.2	2.8	1.4	0.15	0.3	0.14881	0.297619	± 2.8	± 1.4
1.2	2.9	1.45	0.15	0.29	0.143678	0.287356	± 2.9	± 1.45
1.2	3	1.5	0.14	0.28	0.138889	0.277778	± 3	± 1.5
1.2	3.1	1.55	0.14	0.27	0.134409	0.268817	± 3.1	± 1.55
1.2	3.2	1.6	0.14	0.27	0.130208	0.260417	± 3.2	± 1.6
1.2	3.3	1.65	0.13	0.26	0.126263	0.252525	± 3.3	± 1.65
1.2	3.4	1.7	0.13	0.25	0.122549	0.245098	± 3.4	± 1.7
1.2	3.5	1.75	0.12	0.24	0.119048	0.238095	± 3.5	± 1.75
1.2	3.6	1.8	0.12	0.24	0.115741	0.231481	± 3.6	± 1.8
1.2	3.7	1.85	0.12	0.23	0.112613	0.225225	± 3.7	± 1.85
1.2	3.8	1.9	0.11	0.22	0.109649	0.219298	± 3.8	± 1.9
1.2	3.9	1.95	0.11	0.22	0.106838	0.213675	± 3.9	± 1.95
1.2	4	2	0.11	0.21	0.104167	0.208333	± 4	± 2
1.2	4.1	2.05	0.11	0.21	0.101626	0.203252	± 4.1	± 2.05
1.2	4.2	2.1	0.1	0.2	0.099206	0.198413	± 4.2	± 2.1
1.2	4.3	2.15	0.1	0.2	0.096899	0.193798	± 4.3	± 2.15
1.2	4.4	2.2	0.1	0.19	0.094697	0.189394	± 4.4	± 2.2
1.2	4.5	2.25	0.1	0.19	0.092593	0.185185	± 4.5	± 2.25

1.2	1	1	0.42	0.42	0.416667	0.416667	± 1	± 1
1.2	1.1	1.1	0.38	0.38	0.378788	0.378788	± 1.1	± 1.1

1.2	1.2	1.2	0.35	0.35	0.347222	0.347222	± 1.2	± 1.2
1.2	1.3	1.3	0.33	0.33	0.320513	0.320513	± 1.3	± 1.3
1.2	1.4	1.4	0.3	0.3	0.297619	0.297619	± 1.4	± 1.4
1.2	1.5	1.5	0.28	0.28	0.277778	0.277778	± 1.5	± 1.5
1.2	1.6	1.6	0.27	0.27	0.260417	0.260417	± 1.6	± 1.6
1.2	1.7	1.7	0.25	0.25	0.245098	0.245098	± 1.7	± 1.7
1.2	1.8	1.8	0.24	0.24	0.231481	0.231481	± 1.8	± 1.8
1.2	1.9	1.9	0.22	0.22	0.219298	0.219298	± 1.9	± 1.9
1.2	2	2	0.21	0.21	0.208333	0.208333	± 2	± 2
1.2	2.1	2.1	0.2	0.2	0.198413	0.198413	± 2.1	± 2.1
1.2	2.2	2.2	0.19	0.19	0.189394	0.189394	± 2.2	± 2.2
1.2	2.3	2.3	0.19	0.19	0.181159	0.181159	± 2.3	± 2.3
1.2	2.4	2.4	0.18	0.18	0.173611	0.173611	± 2.4	± 2.4
1.2	2.5	2.5	0.17	0.17	0.166667	0.166667	± 2.5	± 2.5
1.2	2.6	2.6	0.17	0.17	0.160256	0.160256	± 2.6	± 2.6
1.2	2.7	2.7	0.16	0.16	0.154321	0.154321	± 2.7	± 2.7
1.2	2.8	2.8	0.15	0.15	0.14881	0.14881	± 2.8	± 2.8
1.2	2.9	2.9	0.15	0.15	0.143678	0.143678	± 2.9	± 2.9
1.2	3	3	0.14	0.14	0.138889	0.138889	± 3	± 3
1.2	3.1	3.1	0.14	0.14	0.134409	0.134409	± 3.1	± 3.1
1.2	3.2	3.2	0.14	0.14	0.130208	0.130208	± 3.2	± 3.2
1.2	3.3	3.3	0.13	0.13	0.126263	0.126263	± 3.3	± 3.3
1.2	3.4	3.4	0.13	0.13	0.122549	0.122549	± 3.4	± 3.4
1.2	3.5	3.5	0.12	0.12	0.119048	0.119048	± 3.5	± 3.5
1.2	3.6	3.6	0.12	0.12	0.115741	0.115741	± 3.6	± 3.6
1.2	3.7	3.7	0.12	0.12	0.112613	0.112613	± 3.7	± 3.7
1.2	3.8	3.8	0.11	0.11	0.109649	0.109649	± 3.8	± 3.8
1.2	3.9	3.9	0.11	0.11	0.106838	0.106838	± 3.9	± 3.9
1.2	4	4	0.11	0.11	0.104167	0.104167	± 4	± 4
1.2	4.1	4.1	0.11	0.11	0.101626	0.101626	± 4.1	± 4.1
1.2	4.2	4.2	0.1	0.1	0.099206	0.099206	± 4.2	± 4.2
1.2	4.3	4.3	0.1	0.1	0.096899	0.096899	± 4.3	± 4.3
1.2	4.4	4.4	0.1	0.1	0.094697	0.094697	± 4.4	± 4.4
1.2	4.5	4.5	0.1	0.1	0.092593	0.092593	± 4.5	± 4.5

1.2	1	1.5	0.42	0.28	0.416667	0.277778	± 1.5	± 1
1.2	1.1	1.65	0.38	0.26	0.378788	0.252525	± 1.65	± 1.1
1.2	1.2	1.8	0.35	0.24	0.347222	0.231481	± 1.8	± 1.2
1.2	1.3	1.95	0.33	0.22	0.320513	0.213675	± 1.95	± 1.3
1.2	1.4	2.1	0.3	0.2	0.297619	0.198413	± 2.1	± 1.4
1.2	1.5	2.25	0.28	0.19	0.277778	0.185185	± 1.5	± 2.25

1.2	1.6	2.4	0.27	0.18	0.260417	0.173611	± 1.6	± 2.4
1.2	1.7	2.55	0.25	0.17	0.245098	0.163399	± 1.7	± 2.55
1.2	1.8	2.7	0.24	0.16	0.231481	0.154321	± 2.7	± 1.8
1.2	1.9	2.85	0.22	0.15	0.219298	0.146199	± 2.85	± 1.9
1.2	2	3	0.21	0.14	0.208333	0.138889	± 3	± 2
1.2	2.1	3.15	0.2	0.14	0.198413	0.132275	± 3.15	± 2.1
1.2	2.2	3.3	0.19	0.13	0.189394	0.126263	± 3.3	± 2.2
1.2	2.3	3.45	0.19	0.13	0.181159	0.120773	± 3.45	± 2.3
1.2	2.4	3.6	0.18	0.12	0.173611	0.115741	± 3.6	± 2.4
1.2	2.5	3.75	0.17	0.12	0.166667	0.111111	± 3.75	± 2.5
1.2	2.6	3.9	0.17	0.11	0.160256	0.106838	± 3.9	± 2.6
1.2	2.7	4.05	0.16	0.11	0.154321	0.102881	± 2.7	± 4.05
1.2	2.8	4.2	0.15	0.1	0.14881	0.099206	± 2.8	± 4.2
1.2	2.9	4.35	0.15	0.1	0.143678	0.095785	± 2.9	± 4.35
1.2	3	4.5	0.14	0.1	0.138889	0.092593	± 3	± 4.5
1.2	3.1	4.65	0.14	0.09	0.134409	0.089606	± 4.65	± 3.1
1.2	3.2	4.8	0.14	0.09	0.130208	0.086806	± 3.2	± 4.8
1.2	3.3	4.95	0.13	0.09	0.126263	0.084175	± 3.3	± 4.95
1.2	3.4	5.1	0.13	0.09	0.122549	0.081699	± 3.4	± 5.1
1.2	3.5	5.25	0.12	0.08	0.119048	0.079365	± 3.5	± 5.25
1.2	3.6	5.4	0.12	0.08	0.115741	0.07716	± 5.4	± 3.6
1.2	3.7	5.55	0.12	0.08	0.112613	0.075075	± 5.55	± 3.7
1.2	3.8	5.7	0.11	0.08	0.109649	0.073099	± 5.7	± 3.8
1.2	3.9	5.85	0.11	0.08	0.106838	0.071225	± 5.85	± 3.9
1.2	4	6	0.11	0.07	0.104167	0.069444	± 6	± 4
1.2	4.1	6.15	0.11	0.07	0.101626	0.067751	± 6.15	± 4.1
1.2	4.2	6.3	0.1	0.07	0.099206	0.066138	± 4.2	± 6.3
1.2	4.3	6.45	0.1	0.07	0.096899	0.064599	± 4.3	± 6.45
1.2	4.4	6.6	0.1	0.07	0.094697	0.063131	± 6.6	± 4.4
1.2	4.5	6.75	0.1	0.07	0.092593	0.061728	± 6.75	± 4.5

LIST OF REFERENCES

[1] S.S. Mahal, ”Effects of Communication Delays on String Stability in an AHS environment,” Master’s Thesis, University of California, Berkeley, March 2000.

[2] J.K. Hedrick, M. Tomizuka, and P. Varaiya, “Control Issues in Automated Highway Systems,” IEEE Control Systems Magazine, 1994.

[3] D.V.A.H.G. Swaroop, ”String Stability of Interconnected Systems: An Application to Platooning in Automated Highway Systems,” Doctor of Philosophy, University of California, Berkeley, April 1994.

[4] Y. Chen, “Effect of Communication Delays on the Performance of Vehicle Platoons,” Master’s Thesis, University of California, Berkeley, May 1995.

[5] D.A. Simakis, “Vehicle Guidance and Control Along Circular Trajectories,” Master’s Thesis, Naval Postgraduate School, Monterey, California, September 1992.

[6] D.L. Lienard, “Autopilot Design for Autonomous Underwater Vehicles Based on Sliding Mode Control,” Engineer’s Thesis, Naval Postgraduate School, Monterey, California, June 1990.

[7] S. Chism, “Robust Path Tracking of Autonomous Underwater Vehicles Using Sliding Mode Control,” Engineer’s Thesis, Naval Postgraduate School, Monterey, California, December 1990.

[8] F.A. Papoulias, “On the Nonlinear Dynamics of Pursuit Guidance for Marine Vehicles,” Journal of Ship Research, vol.37, no.4, p.342-353, Dec. 1993.

[9] F.A. Papoulias, “Dynamics of Marine Vehicles,” Lecture notes, NPS, Monterey California, 1993.

[10] F.A. Papoulias, “Cross Track Error and Proportional Turning Rate Guidance of Marine Vehicles,” Journal of Ship Research, vol.38, p.123, 1994.

THIS PAGE INTENTIONALLY LEFT BLANK

INITIAL DISTRIBUTION LIST

1. Defense Technical Information Center
   Ft. Belvoir, Virginia

2. Dudley Knox Library
   Naval Postgraduate School
   Monterey, California

3. Fotis Papoulias
   Department of Mechanical and Aerospace Engineering
   Naval Postgraduate School
   Monterey, California

4. Oleg Yakimenko
   Department of Mechanical and Aerospace Engineering
   Naval Postgraduate School
   Monterey, California